Memoirs of the Faculty of Engineering, Nagoya University
Vol. 28, No. 2. (1976)

Crystallization of Coesite

SHIGEHARU NAKA, SUKETOSHI ITO, TETSUYA KAMEYAMA
and MICHIO INAGAKI

Synthetic Crystal Research Laboratory

(received October 30, 1976)

CONTENTS

1. General Introduction 266
2. Experimental Procedure 270
2. 1. High-Pressure Apparatus 270
2. 2. Starting Materials 273
2. 3. Treatments under High Pressure and High Temperature 273
2. 4. Techniques for Characterization 274
3. Quartz-Coesite Phase Boundary 274
3. 1. Introduction 274
3. 2. Experimental 275
3. 3. Results and Discussion 275
4. Kinetic Studies of Crystallization of Coesite 278
4. 1. Introduction 278
4. 2. Experimental 278
4. 3. Results 279
4. 3. 1. Crystallization Kinetics of Coesite from Amorphous Silica 279
4. 3. 2. Crystallization Kinetics of Coesite from Quartz 281
4. 4. Discussion 283
4. 4. 1. Kinetic Process of Crystallization of Coesite from Amorphous Silica 283
4. 4. 2. Kinetic Process of Crystallization of Coesite from Quartz 285
4. 4. 3. Effect of Starting Material on Rate of Crystallization of Coesite 285
5. Morphological Development of Coesite 285
5. 1. Introduction 285
5. 2. Experimental 286
5. 3. Results and Discussion 286
5. 3. 1. Morphology of Crystals formed from Amorphous Silica 286
5. 3. 2. Morphology of Crystals formed from Quartz 291
6. Crystallization of Coesite from Various Starting Materials in the Presence of Water 293
6. 1. Introduction 293
6. 2. Experimental 294
6. 3. Results 294
6. 3. 1. Crystallization Kinetics of Coesite from Amorphous Silica 294

6. 3. 2. Crystal Morphology of Quartz and Coesite formed from Amorphous Silica 296
6. 3. 3. Crystallization Kinetics of Coesite from Silica Glass and Crystal Morphology 299
6. 3. 4. Crystallization Kinetics of Coesite from Quartz and Crystal Morphology 301
6. 4. Discussion 302
6. 4. 1. Effect of Water on Crystallization of Coesite 302
6. 4. 2. Crystallization of Coesite in the Relation to the Solid-Liquid Boundary of Water 305
7. Twinning in Coesite 306
7. 1. Introduction 306
7. 2. Experimental 306
7. 3. Results and Discussion 306
8. Crystal Growth of Coesite 309
8. 1. Introduction 309
8. 2. Experimental 310
8. 3. Results and Discussion 310
9. Conclusive Remarks 313
Acknowledgement 315
References 315

Chapter 1. General Introduction

Silica, SiO_2, is well known to have three principal crystalline phases under normal pressure; quartz, tridymite and cristobalite. All of them consist of three-dimensional networks of SiO_4 tetrahedra in different ways for different phases, and they have rather porous, not close packed, structures. Therefore, it had been expected that they transform to a denser structure under high pressure. Coes (1953) have succeeded to get a high-pressure phase from quartz under the pressure of more than 35 kbars at 500 ~ 800 ℃ in a piston-cylinder-type high-pressure apparatus. It has about 10 % higher density (d=2.92 g/cm^3) than quartz (d=2.65 g/cm^3) and belongs to monoclinic system, which is called "coesite" after the discoverer. This new phase also consist of SiO_4 tetrahedra, and its structure is different from the one estimated from the analogy to the oxides of germanium and tin, which belong to the same group of Periodic Table. Later, Dachille and Roy (1959) have showed that high pressure modification of BeF_2, which is known as a weakened model of silica, has the same structure as coesite, and consequently confirmed that coesite is the stable phase under high pressure. The phase isomorphous with rutile, which is expected from Periodic Table and has SiO_6 octahedra, has been synthesized at 1200 ~ 1400℃ under the pressure of more than 120 kbars (Stishov and Popova, 1961) and is called "stishovite". Its structure is much denser than coesite (d=4.28 g/cm^3). After the successes of synthesis, both coesite and stishovite have been found in nature; in the sandstone collected from Meteor Crater, Arizona (Chao, et al. 1960 and 1962).

The stability, crystallographic structure and optical properties of coesite have mainly been studied. In Table 1. 1, the unit cell parameters and optical properties are summarized, according to Sclar et al. (1962). The structure of coesite is compared with that of low-quartz in Fig. 1. 1 by illustrating the projections along the c-axis.

Table 1. 1. Unit cell parameters and optical properties of coesite.

density	2.915±0.005 (measured), 2.919± (calculated)
lattice parameter	a = 7.14±0.01 Å, b= 12.37±0.01 Å, c = 7.14±0.01 Å, β = 120°.
unit cell volume	546 Å^3
z	16
indices of refraction	α = 1.5940, β = 1.5955, γ = 1.5990. $\gamma - \alpha$ = 0.005±0.001
optic sign	(+)
optic angle	64° (measured), 66°44′ (calculated)
dispersion	horizontal with $\gamma < v$ (weak)
optical orientation	X = b, Z∧c = 4 ~ 6°, β = 120°
twinning	simple contact twins with twin and composition plane of (021)
habit	hexagonal platelets and euhedral to subhedral laths with (+) elongation and parallel extinction
color	colorless
luster	vitreous
cleavage	non, subconcoidal fractures

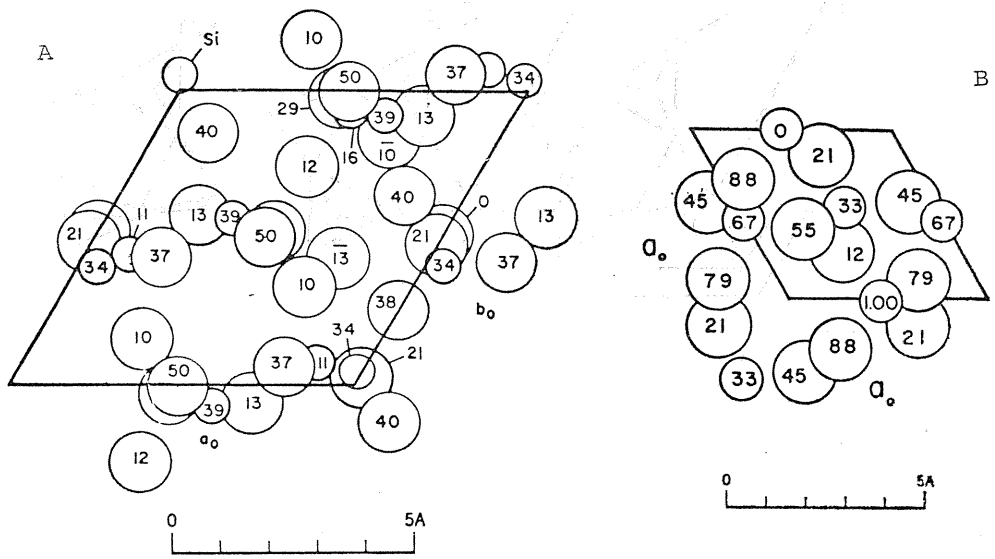

Fig. 1. 1. A projection along the c-axis (Wycoff, 1963)
(A) coesite, (B) low-quartz.

Coesite belongs to the space group of C2/c in the monoclinic system (Zoltai & Buerger, 1959; Araki & Zoltai, 1969). The lattice parameters a and c are practically the same with each other and β equals to 120°. Therefore, it can be said pseudohexagonal and the crystal habits observed on synthetic coesite are similar to those observed on hexagonal crystals (Sclar et al., 1962). The fundamental unit of the structure is a ring which consists of four SiO_4-tetrahedra. In coesite, these rings are connected along the direction of <110> on the (001) plane and also along <001> direction on the (010) plane by sharing the corner of SiO_4-tetrahedra. In Fig. 1. 2, the chains of the rings of four SiO_4-tetrahedra along the <001> direction are shown on the plane of (010). These chains are bridged by another rings (showed only one ring hatched, for an example, in the figure). In quartz, on the other hand, the rings of four SiO_4-tetrahedra are connected by sharing the tetrahedron along the <100> direction and the chain of rings with six-fold screw are formed by sharing the corner of the tetrahedron along the <001> direction.

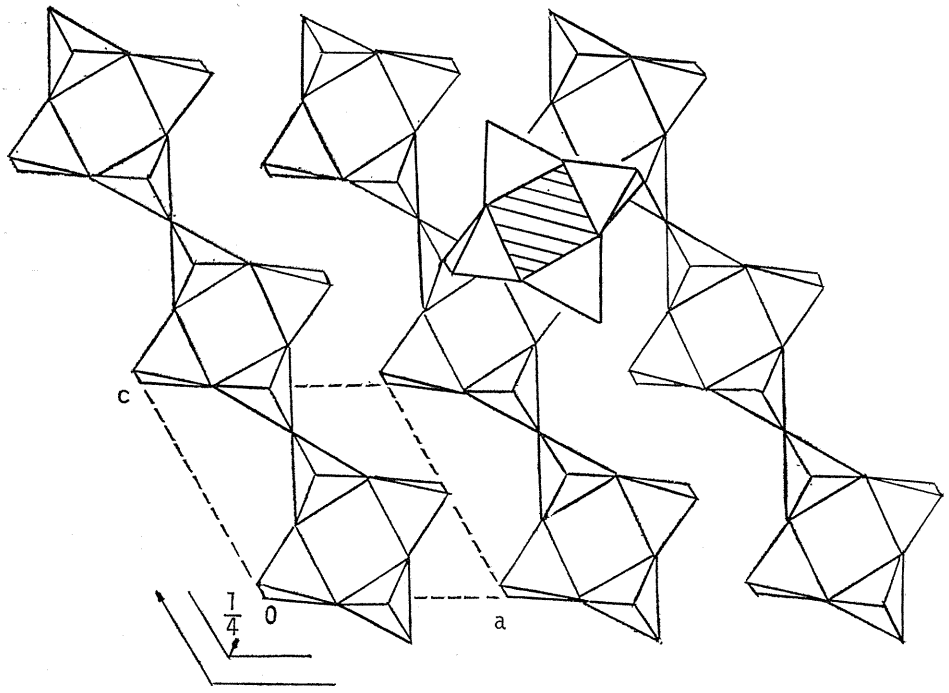

Fig. 1. 2. Chains of the rings of four SiO_4-tetrahedra on the (010) plane of coesite (Araki & Zoltai, 1969).

The physico-chemical properties of coesite are not known well yet. It is noteworthy, however, that coesite has rather high resistance to hydrofluoric acid.

The phase diagram of silica is shown in Fig. 1. 3. The phase boundaries between α- and β-quartz are those reported by Yoder (1950) and Cohen and Klement (1697). The boundary between coesite and stishovite is after Akimoto and Syono (1966). On the boundary between quartz and coesite, however, there have been reported by many authors using different high-pressure apparatus. In Fig. 1. 3,

the boundaries reported by Boyd and England (1960) and by Griggs and Kennedy (1956) are drawn, the former being obtained in the piston-cylinder-type apparatus and the latter in the ooposed-anvil-type apparatus. As shown by these two boun-

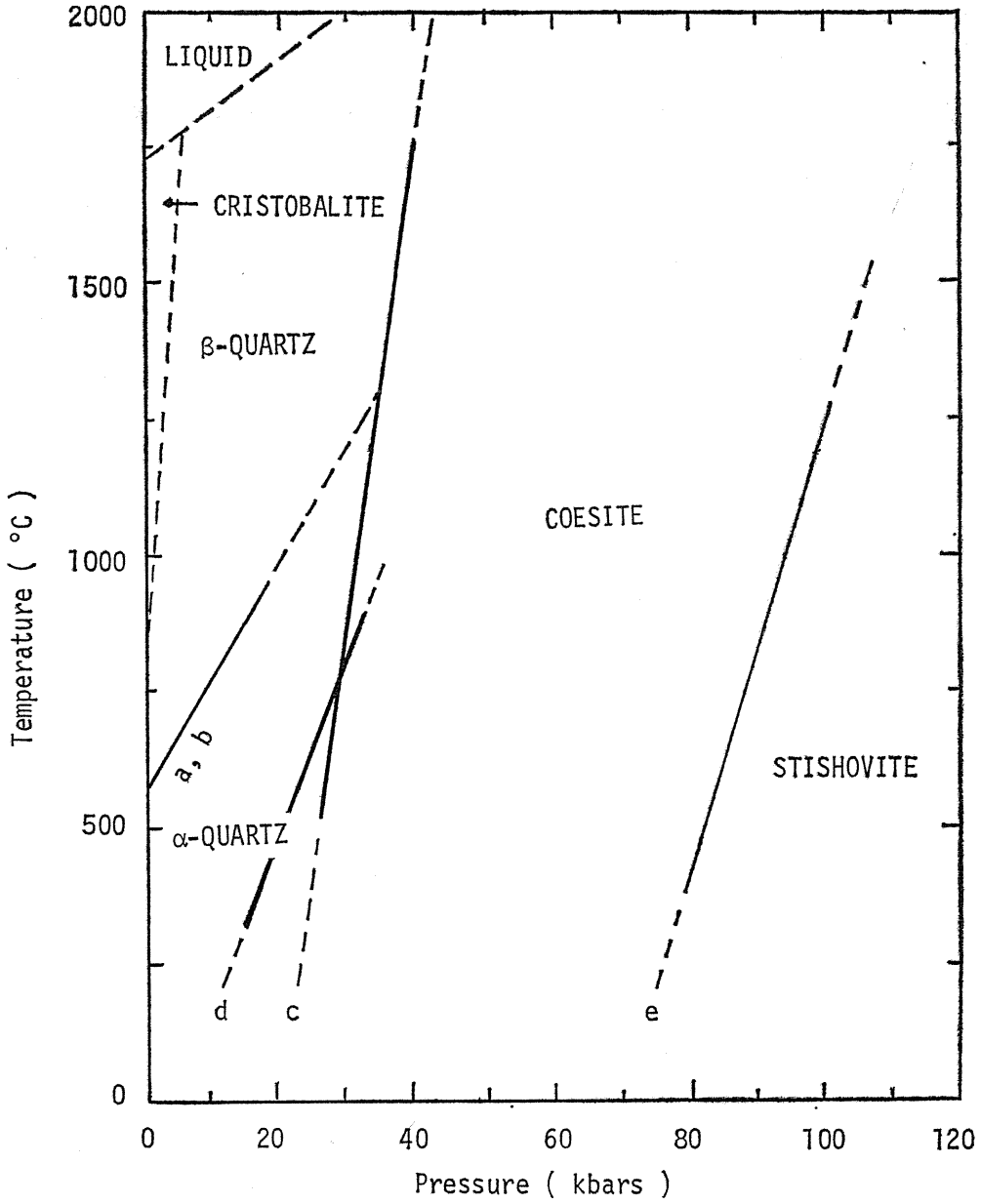

Fig. 1. 3. Phase diagram of silica.
a: Yoder (1950), b: Cohen & Klement (1967),
c: Boyd & England (1960), d: Griggs & Kennedy (1956),
e: Akimoto & Syono (1969).

daries and disussed in detail in following chapter, the boundaries observed do not coincide with each other. These wide dispersion of the experimental results may be due to the difference in stress gradient in the sample, in other words, the difference in shear exerted on the sample. The physico-chemical environment of the sample seems to give certain effect on the reconstructive transition of silica. Therefore, it is necessary to determine the boundary and stable region of coesite by taking into consideration of these different factors; apparatus, shear, environment, etc.

The purposes of the present work are *the systematic studies of crystallization of coesite in the girdle-type high-pressure apparatus which has been developed in our laboratory and the presentation of fundamental information on high-temperature and high-pressure solution growth of coesite.*

The present paper is composed of nine chapters; in Chapter 1, a short summary of the structure and properties of coesite were presented. The girdle-type high-pressure apparatus used, the starting materials and the techniques for characterization were explained in Chapter 2. In Chapter 3, the determination of the phase boundary between quartz and coesite in the girdle-type high-pressure apparatus and the discussion on the effect of shear on the boundary were described. The kinetics of crystallization of coesite from amorphous silica and quartz under various tempereture-pressure conditions were studied and the morphological development of crystals of coesite and metastable quartz during crystallization was examined under polarizing microscope, in Chapter 4 and 5, respectively. The effects of pressure and temperature on crystallization rate and crystal morphology were discussed. In Chapter 6, the kinetics and morphological development of coesite from various starting materials were studied in the presence of water under pressures. The effect of water was discussed in comparison with the results under anhydrous condition. Two penetration twins which were found in the present work were described and the mechanism of their formation was discussed in Chapter 7. The preliminary experiments of single crystal growth of coesite were also performed in the presence of distilled water and 0.5 N NaOH solution (Chapter 8). And in the last Chapter, a summary of the results of the present work was presented.

Most of the resluts presented here have been reported separately in different journals; Journal of American Ceramic Society (Naka et al., 1972b; 1974; Kameyama & Naka, 1974), J. Crystal Growth (Naka et al., 1974), American Mineralogist (Naka et al., 1975), Bulletin of Chemical Society of Japan (Kameyama et al., 1976) and Chemistry Letters (Naka et al., 1974). Here, we hope to present the comprehensive understanding of the crystallization of coesite under various conditions by summarizing and reviewing our results published separately and by giving unpublishd results and discussion.

Chapter 2. Experimental Procedure

2. 1. High-Pressure Apparatus

Among the high-pressure apparatus developed, the so-called girdle-type one (Daniels & Jones, 1961; Bundy, 1962; Young et al., 1963; Nichols, 1969) is powerfull for the syntheses of inorganic materials under high pressures because of facility of obtaining very high pressure and also because of relatively large volume of sample, in spite of the lack of strict homogeneity of pressure in sample cell (Naka et al.,

1972a). In the present work, the girdle-type high-pressure apparatus, of which the cone half angle was 45°, was used. A composite gasket of pyrophyllite, steel and teflon was selected on the basis of the detailed examinations on the cell arrangement, gasket, the maximum pressure attainable and pressure distribution in the cell (Naka et al., 1972a). In Figs. 2. 1 and 2. 2, the schematic illustrations of the girdle-type apparatus used are shown. The bore diameter of the cylinder is larger than diameter of the top of the conical piston. By using the cell arrangment shown in Fig. 2. 1 (the bore diameter of the cylinder is 12 mm and the diameter of the piston is 8 mm), stable pressures between 15 and 60 kbars were obtained rather easily and the long life of the cell was attained. For the experiments above 60 kbars pressure, the cell arrangement shown in Fig. 2. 2 was used, in which two disks of tungsten carbide and steel were inserted. The bore diameter of the cylinder was 16 mm and the diameter of the piston was 12 mm, but the volume of the sample kept the same as that in Fig. 2. 1. In these arrangements, the pressure exerted on the center of the sample has been found to be 10 ~ 15% larger than that on the end of the sample. The stress was concentrated to the sample. The increase of the thickness of the disks increased the degree of stress concentration and resulted in the increase of pressure attainable.

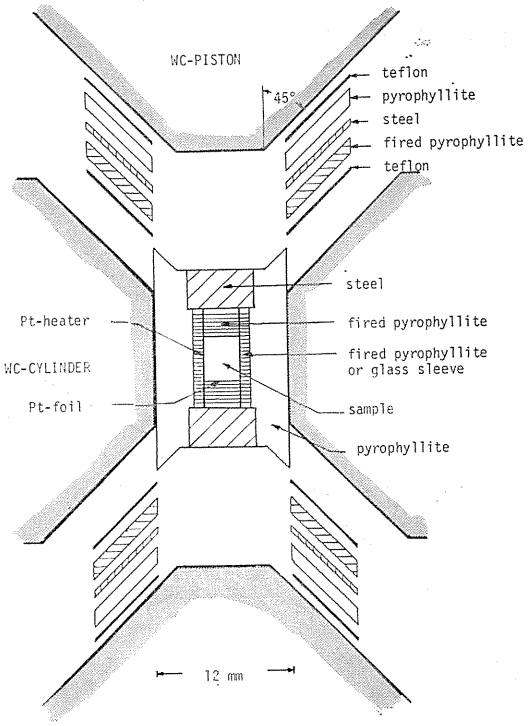

Fig. 2. 1. Schematic illustration of the girdle-type high-pressure apparatus used.

The pressure calibration for the cell arrangements shown in Figs. 2. 1 and 2. 2 was performed by detecting the changes of electrical resistance during polymorphic transitions of the reference metal wires, Bi, Tl, and Ba. In Fig. 2. 3, the calibration curves for the cell arrangements used in the present work are shown as the relation

between pressure exerted on the sample and load of the oil press. The transition points of the reference metal are the values reported by National Bureau of Stan-

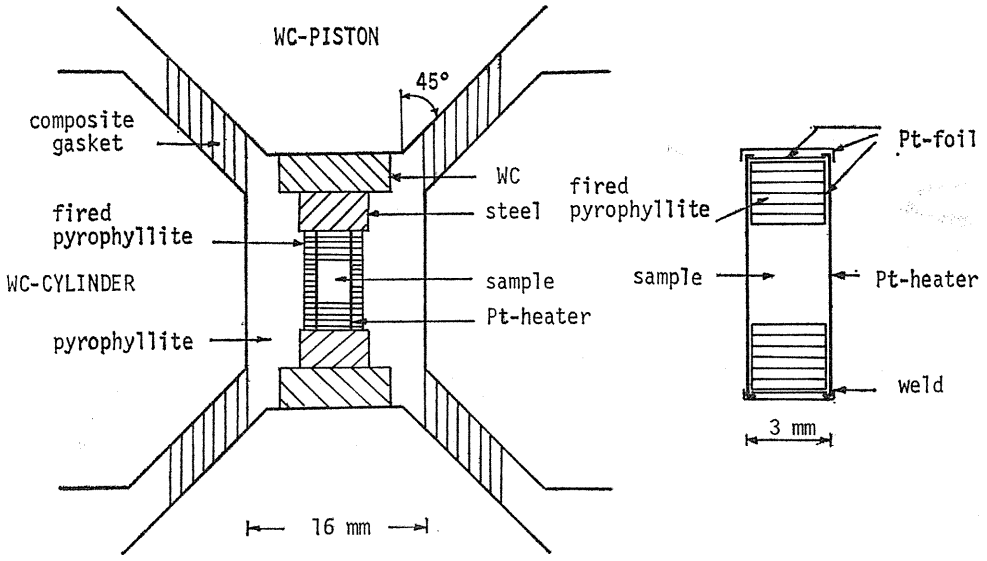

Fig. 2. 2. Cell arrangement in the girdle-type apparatus. The platinum container is also shown to illustrate the detailed construction.

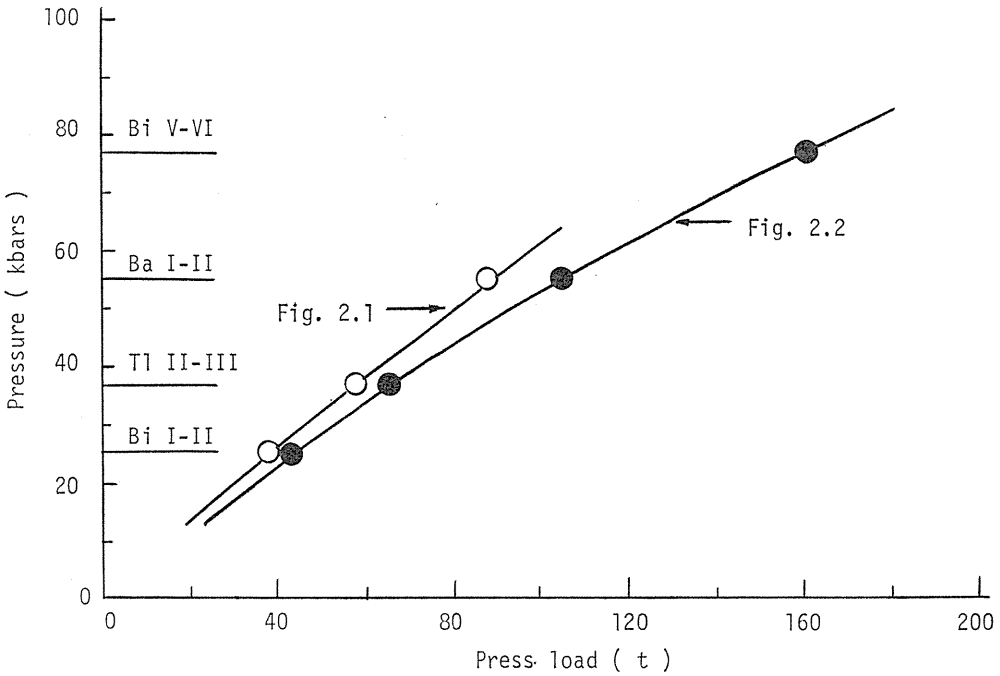

Fig. 2. 3. The relations between pressure and load of the oil press for two cell arrangements used.

dards (1968); Bi I-II: 25. 5 kbars, Tl II-III: 36.7±0.3 kbars, Ba I-II: 55±2 kbars, and Bi V-VI: 77±3 kbars. The accuracy of the pressure determination was thought to be ≈ ± 4 %.

The temperature of the sample under pressure was estimated from the electrical input power by using a calibration curve which had been determined with a Chromel-Alumel thermocouple placed in the center of the sample. The relation between input power and temperature obtained up to ≈ 1100 ℃ using the thermocouple was corrected for the melting points of Au and Ni (1235 ℃ and 1138 ℃ under 30 kbars, respectively (Cohen et al., 1966)), measured with the same cell arrangements.

2. 2. Starting Materials

The starting materials used in the present work were noncrystalline silicas (so-called amorphous silica and silica glass), quartz and cristobalite. The method and condition of preparation of these starting materials are shown below;

1. Amorphous silica A: prepared by heating the silica gel at 1200℃ for 2 h, which was made by hydrolysis of the reagent-grade silicon tetrachloride at room temperature. Its particle size was less than 50 μm.
2. Amorphous silica B: prepered by the same procedure, but using the reagent-grade silicon ethoxide. The particle size was 0.1 ~ 10 μm.
3. Silica glass: prepared by mechanical grinding of the commercial silica glass rods. After grinding, the powder with the particle size of 0. 5 ~ 1. 0 μm was taken by means of elutriation and then heated at 800℃ for 2 h in order to remove the strain and absorbed water.
4. Quartz A: obtained from a natural quartzite which was heated at 800 ℃ for 1 h. The chemical composition was reported as follows; 99.55 % SiO_2, 0. 17 % Al_2O_3, 0. 02 % Fe_2O_3, 0. 05 % CaO and 0. 18 % ignition loss. The particle size was limited to 7 ~ 15 μm.
5. Quartz B: prepared from the synthetic quartz lump by mechanical grinding and heated at 800 ℃ for 48 h in order to remove the absorbed water. The particle size was 0. 5 ~ 1. 0 μm.
6. Cristobalite: prepared by the same procedure as the amorphous silica B. The particle size was 10 ~ 20 μm.

All six kinds of starting materials were kept in the desiccator.

2. 3. Treatments under High Pressure and High Temperature

After the starting material is set in the cell of the high-pressure apparatus, it was compressed up to a desired pressure (15 ~ 90 kbars) at room temperature. The sample was heated with the heating rate of 200 ℃/min by increasing the input power for the platinum heater, and after a programmed duration (3 min ~ 200 h) at a desired temperature (100 ~ 1600 ℃) quenched in the cell under compression.

The treatment of the sample were not only under anhydrous conditions but also under hydrous conditions; in the presence of distilled water and of 0. 5 N NaOH solution. After mounting the sample powder in the platinum container, few drops of water were added. The amount of water was determined from the number of drops added. The shielding of the water in the container was successfully performed by overlapping the platinum foils, as illustrated in Fig. 2. 2. It was confirmed that about 80 ~ 90 % of the added water remained in the sample container after the treatmet at 900 ℃ under 30 kbars pressure for 72 h.

2. 4. Techniques for Characterization

After the sample was heated under compression, it was examined by X-ray powder diffraction techniques to identify the phases and to determine the proportions of the phases. The specimen for X-ray analysis and microscopy was taken from the central part (1 mm thick) of the treated sample to avoid serious effects of the large temperature and pressure gradients along the cylinder axis (Naka et al., 1972a) on the results.

A recording goniometer with a scintillation counter and pulse height analyzer and Ni-filtered Cu Kα radiation were used. The ratio of amorphous phase to crystalline phase was evaluated from the diffraction intensity measured at 22.5° in 2θ, the maximum position for amorphous silica. The ratio of coesite to quartz was determined from the integrated intensity ratio of the 040 to the 101 diffraction line. The relative proportions of amorphous silica, quartz, and coesite were normalized to a sum of 100 %. The estimated error of repeated determination was about ± 5 % in quantification of amorphous silica and about ± 2 % in quartz and coesite. The proportions determined by X-ray analysis agreed well with microscopic observations. The size L and lattice strain ε of crystallite were determined from half widths of X-ray diffraction lines according to Hall's equation;

$$\frac{\beta \cos \theta}{\lambda} = \frac{K}{L} + 2\varepsilon \frac{\sin \theta}{\lambda}, \tag{2.1}$$

where K is the shape factor, λ the wavelength of radiation used and θ the Bragg angle.

The crystals formed by treatments under high-pressure and high-temperature were observed under polarizing microscope by using either thin section or powder as-obtained. The crystals of quartz and coesite were differentiated from amorphous silicas under crossed nicols, and coesite was detected from quartz under open nicol because of its high refractive indices in comparison with quartz. The orientation of optical axes of twins of coesite was decided by using thin section under crossed nicols and universal stage. The twin plane was determined from the stereographic projections.

The observation under scanning electron microscope was performed on the as-obtained samples, either sintered or powder, after coating of gold film on the sample holder.

Chapter 3. Quartz-Coesite Phase Boundary

3. 1. Introduction

Reconstructive transitions among cristobalite, tridymite and quartz are known to be strongly influenced by pressure, nonuniformity of stress, grain size, and also by chemical environment (Sosman, 1965). The density of a quartz glass after compression depends strongly on the pressure-transmitting medium used in the pressure cell; remarkable densification has resulted under the condition in which there was a large external shear (Mackenzie, 1963).

The quartz-coesite phase boundary has been studied with quenching method using the simple-anvil apparatus (Griggs & Kennedy, 1956; MacDonald, 1956; Dachille &

Roy, 1959; Roy & Frushour, 1971), the piston-cylinder apparatus (Boyd & England, 1960; Kitahara & Kennedy, 1964; Green et al., 1966; Boyd et al., 1967), and the tetrahedral-anvil apparatus (Takahashi, 1963). The phase boundaries reported, however, do not coincide with each other. The discrepancy between the boundaries reported seems to result from the differences in shear which are not only due to the scheme of pressure production in various apparatus but also due to the detailed cell arrangement used in the apparatus. In the pressure cell of the girdle-type apparatus, a large stress gradient has been expected, larger than in that of piston-cylinder and multi-anvil apparatus (Naka et al., 1972a). In this chapter, therefore, we determined the boundary between quartz and coesite in the pressure cell of the girdle-type high-pressure apparatus which was used in the following experiments on crystallization of coesite. The distribution of pressure in the cell was changed by adding water to the sample and by using different pressure-transmitting media around the sample in order to understand the effect of shear on the transition between quartz and coesite.

3. 2. Experimental

The pressure cell used was shown in Fig. 2. 1. In the present work, three series of experiments were carried out by using the calcined pyrophyllite sleeve around the sample with 10 wt% of water and without water, and also by using a boro-silicate glass sleeve in the place of the calcined pyrophyllite. The pyrophyllite sleeve and disks around the sample were calcined and dehydrated at 800 ℃ for 1 h. The samples were heated under a given pressure for 1 to 10 h below 1000 ℃ and for 1/2 to 1 h above 1000 ℃, and quenched under compression in the apparatus. The existing phases were then identified by X-ray powder diffractometry using CuKα radiation and by optical microscopy. The starting material was a natural quartz, quartzite, denoted as "quartz A" in Chapter 2. The synthetic coesite was also used as a starting material.

3. 3. Results and Discussion

The quartz-coesite equilibrium lines are shown in Fig. 3. 1-A ~ -C, which are obtained without the addition of water by using pyrophyllite sleeve (dry sample with pyrophyllite sleeve) and using glass sleeve (dry sample with glass sleeve), and with 10 wt % of water by using pyrophyllite sleeve (wet sample).

The equilibrium line obtained for the dry sample with pyrophyllite sleeve above 1100 ℃ was approximately parallel to that for the wet sample, probably due to the softening of the pyrophyllite around the sample above that temperature. Below 1100 ℃, however, the line for the dry sample with pyrophyllite sleeve was displaced remarkably to lower pressure. For the dry sample with glass sleeve, the equilibrium line above the melting point of the glass (about 900 ℃) was found to lie between those for the dry sample with pyrophyllite sleeve above 1100 ℃ and for the wet sample. The presence of liquid seemed to increase the hydrostaticity in pressure exerted on the sample, in other words, to reduce shear in the sample, as did the softening of the pressure-transmitting medium at high temperatures. Below 1100 ℃, on the other hand, there seemed to be a large shear in the dry sample with pyrophyllite sleeve, resulting from the large stress gradient in the pressure-transmitting medium. This shear may lower the equilibrium pressures as is evident in Fig. 3. 1-A.

The equilibrium lines previously reported, including the results of the present work are summarized in Fig. 3. 2. The equilibrium line obtained for the wet

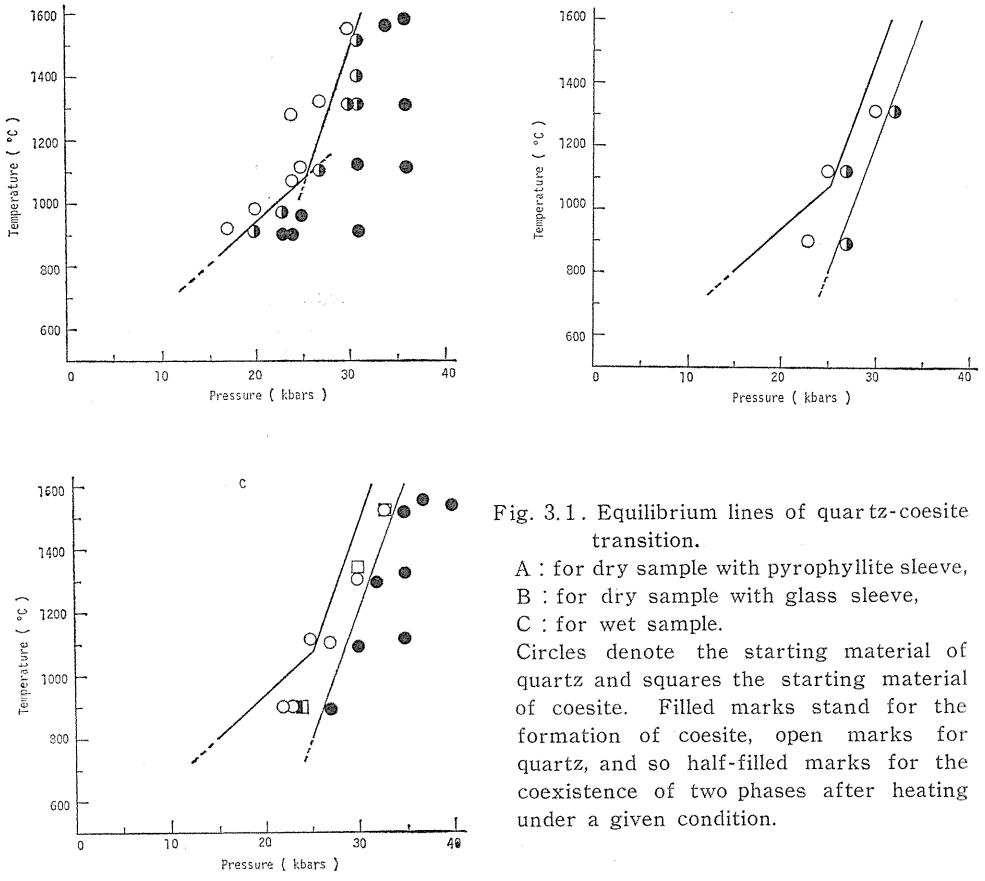

Fig. 3.1. Equilibrium lines of quartz-coesite transition.
A : for dry sample with pyrophyllite sleeve,
B : for dry sample with glass sleeve,
C : for wet sample.
Circles denote the starting material of quartz and squares the starting material of coesite. Filled marks stand for the formation of coesite, open marks for quartz, and so half-filled marks for the coexistence of two phases after heating under a given condition.

sample (curve 10) has almost the same slope as those obtained under hydrostatic pressure condition in the piston-cylinder and multi-anvil apparatus. The assumption that the shear in the sample lowers the equilibrium pressure may be supported by the fact that the equilibrium line for the dry sample below 1100 ℃ has almost the same slope as that obtained under non-hydrostatic pressure condition in the simple-opposed-anvil apparatus. Böhler & Arndt (1974) determined directly the phase transition between quartz and coesite with *in situ* X-ray powder diffraction technique under high-pressure and high-temperature, and obtained for equilibrium line which coincided well with the calculated one (curve 11 in Fig. 3. 2). They attributed the discrepancy among the equilibrium lines reported previously to the uncertainty about pressure produced in various apparatus at high temperatures. As pointed out by Ubbelohde (1957), however, the effect of the circumstance, for example strain energy, has to be taken into consideration on the phase transition between condenced phases. The present results which have been obtained by using the same apparatus with different cell arrangement show the importance of shear on the phase transition A metastable growth of coesite on highly strained quartz reported by Green (1972) agrees with the present result that shear shifts the equilibrium line toward lower pressure.

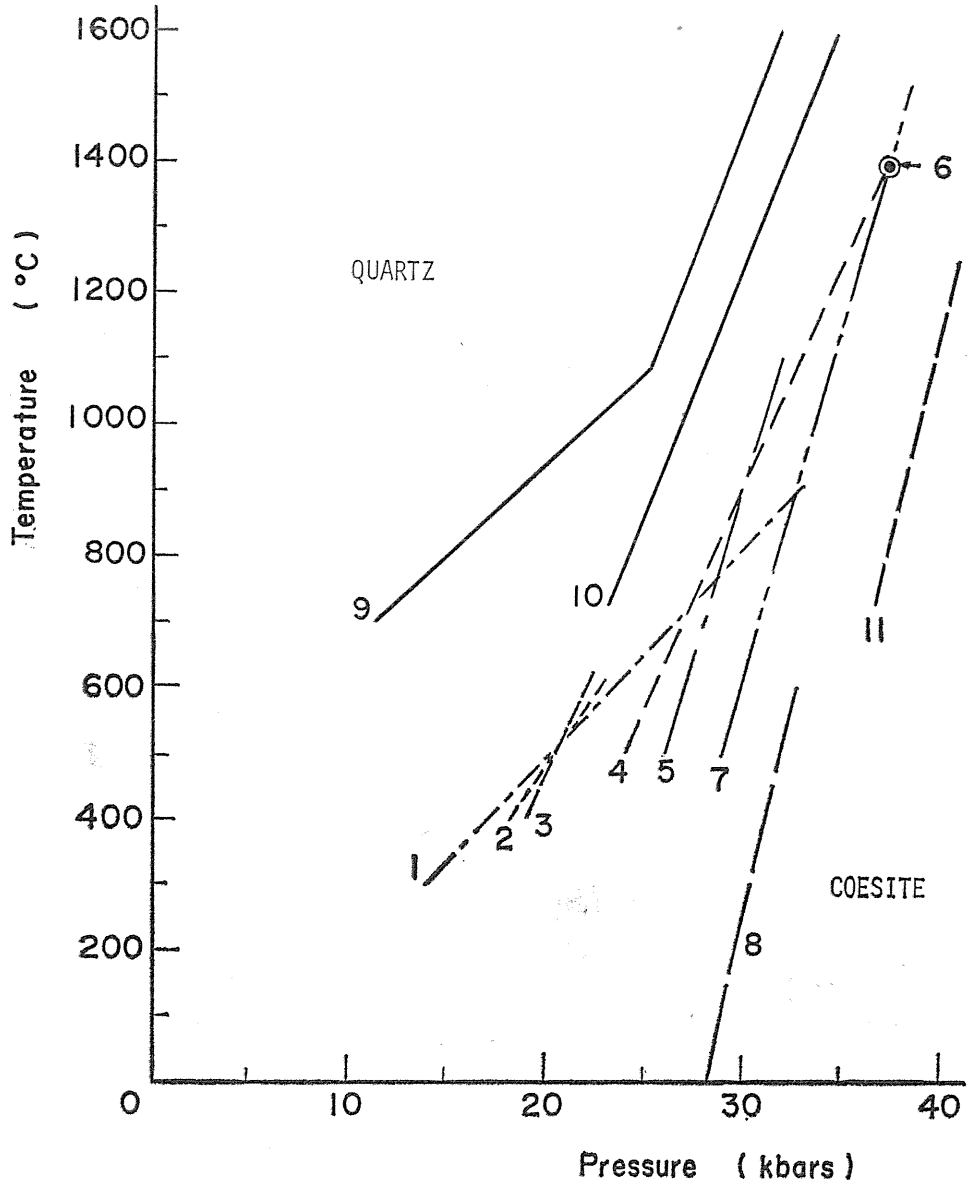

Fig. 3. 2. Equilibrium lines obtained with various apparatus.

1~4: simple-anvil,
5~6: piston-cylinder,
7: tetrahedral-anvil,
8: calculated,
9~10: girdle-type,
11: belt-type

1: Griggs & Kennedy, 1956,
2: MacDonald, 1956,
3: Dachille & Roy, 1959,
4: Roy & Frushour, 1971,
5: Kitahara & Kennedy, 1964,
6: Boyd et al., 1967,
7: Takahashi, 1963,
8: Holm et al., 1967,
9: present work for dry sample,
10: present work for wet sample,
11: Böhler & Arndt, 1974.

Chapter 4. Kinetic Studies of Crystallization of Coesite

4. 1. Introduction

Generally speaking, the stable phase formed under a given condition is not the phase which is most likely to appear first, as stated by Ostwald's step rule (Sosman, 1965). This is the case in the reconstructive transitions of silica which are very sluggish and are influenced by various experimental factors. When quartz transforms to cristobalite, an intermediate glassy phase with a density of 2.30 g/cm^3 is observed from 1400 ℃ to 1650 ℃ (Chaklader & Roberts, 1961). A short-range-ordered amorphous intermediate phase (Skinner & Fahey, 1963) was reported in the reversal transitions of stishovite and coesite to less dense phases under atmospheric and high pressures (Dachille et al., 1963; Gigl & Dachille, 1968). According to Livshits et al. (1972), however, coesite can transform to quartz without formation of any intermediate phase under atmospheric pressure to 25 kbars at temperatures up to 1000 ℃. When amorphous silica and other phases transform to coesite, quartz is found as a metastable phase (MacDonald, 1956; Dachille & Roy, 1959; Boyd & England, 1960; Kitahara & Kennedy, 1964; Uhlmann et al., 1966; Naka et al., 1972b). Quartz is converted to an amorphous phase by shock compression (De Carli & Jamieson, 1959).

In the present chapter, we described the results of kinetic studies of crystallization of coesite. The transition from amorphous silica and quartz to coesite were kinetically studied under various pressure-temperature conditions in the absence of water. The crystallization process of coesite was explained by a consecutive rate process from amorphous silica through quartz to coesite. The stability of intermediate quartz phase is discussed in relation to pressure and temperature.

4. 2. Experimental

The used cell arrangement of the girdle-type high-pressure apparatus was the one shown in Fig. 2. 1.

The starting materials were amorphous silica and quartz. The amorphous silica was prepared by hydrolysis of $SiCl_4$ and the details on it was described in Chapter 2 as "amorphous silica A". Quartz was a natural quartzite, "quartz A" in Chapter 2.

The crystallization of coesite was carried out by using dry sample under the pressures of 23 ~ 55 kbars at the temperatures of 550 to 900 ℃ for the various holding times from 3 to 580 min. These experimental pressure-temperature conditions are within the equilibrium field of coesite, as shown in Fig. 4. 1. The phase boundary between quartz and coesite has been determined in exactly

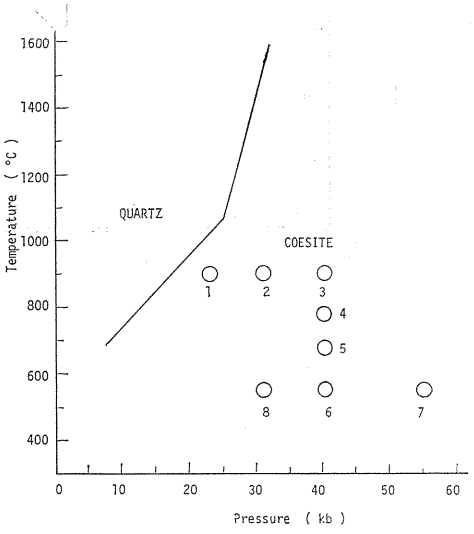

Fig. 4. 1. Experimental pressure-temperature conditions in relation to phase boundary between quartz and coesite for the dry sample.

the same cell arrangement and dry quartz sample (Chapter 3).

4. 3. Results

4. 3. 1. Crystallization Kinetics of Coesite from Amorphous Silica

The variations with time in the proportions of amorphous silica, quartz and coesite at constant temperatures under various pressure are shown in Fig. 4. 2-A and -B.

At 550 ℃ under 40 kbars (Fig. 4. 2-A) the amount of amorphous silica decreases with increasing time, but the amount of quartz reaches a maximum at about 150 min. After passing through this maximum of quartz, the amount of coesite increases abruptly. Under 55 kbars at 550 ℃, however, only a trace of quartz is detected, and coesite is formed much more slowly than at the same temperature under 40 kbars pressure. Under 31 kbars at 550 ℃, on the other hand, a relatively large amount of quartz is found and the formation of coesite is again slower than under 40 kbars.

At 900 ℃ (Fig. 4. 2-B), amorphous silica disappears much more quickly under the pressures examined, and therefore only quartz and coesite phases are found in the samples heat-treated. Under 31 kbars pressure, almost 100 % conversion to quartz is observed only after 5 to 10 min, followed quickly by the formation of coesite. The intermediate phase of quartz is rather stable at 23 kbars and begins to transform to coesite only after it is heated for 450 min.

In Fig. 4. 2-C, the variations in the proportions of the three phases, amorphous silica, quartz and coesite, at different temperatures under a constant pressure of 40 kbars are shown.

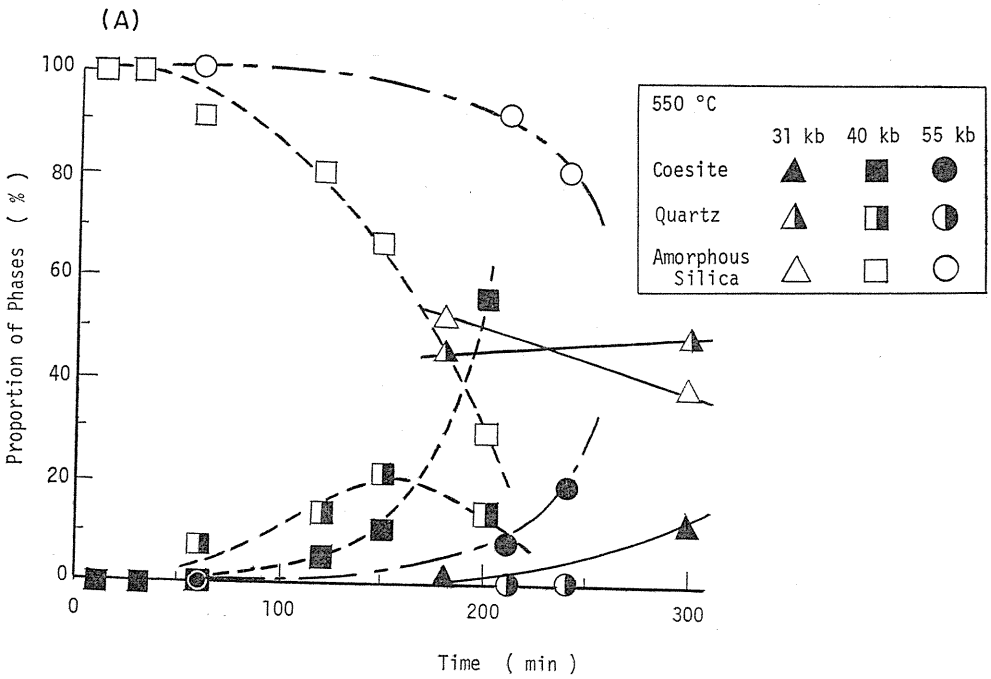

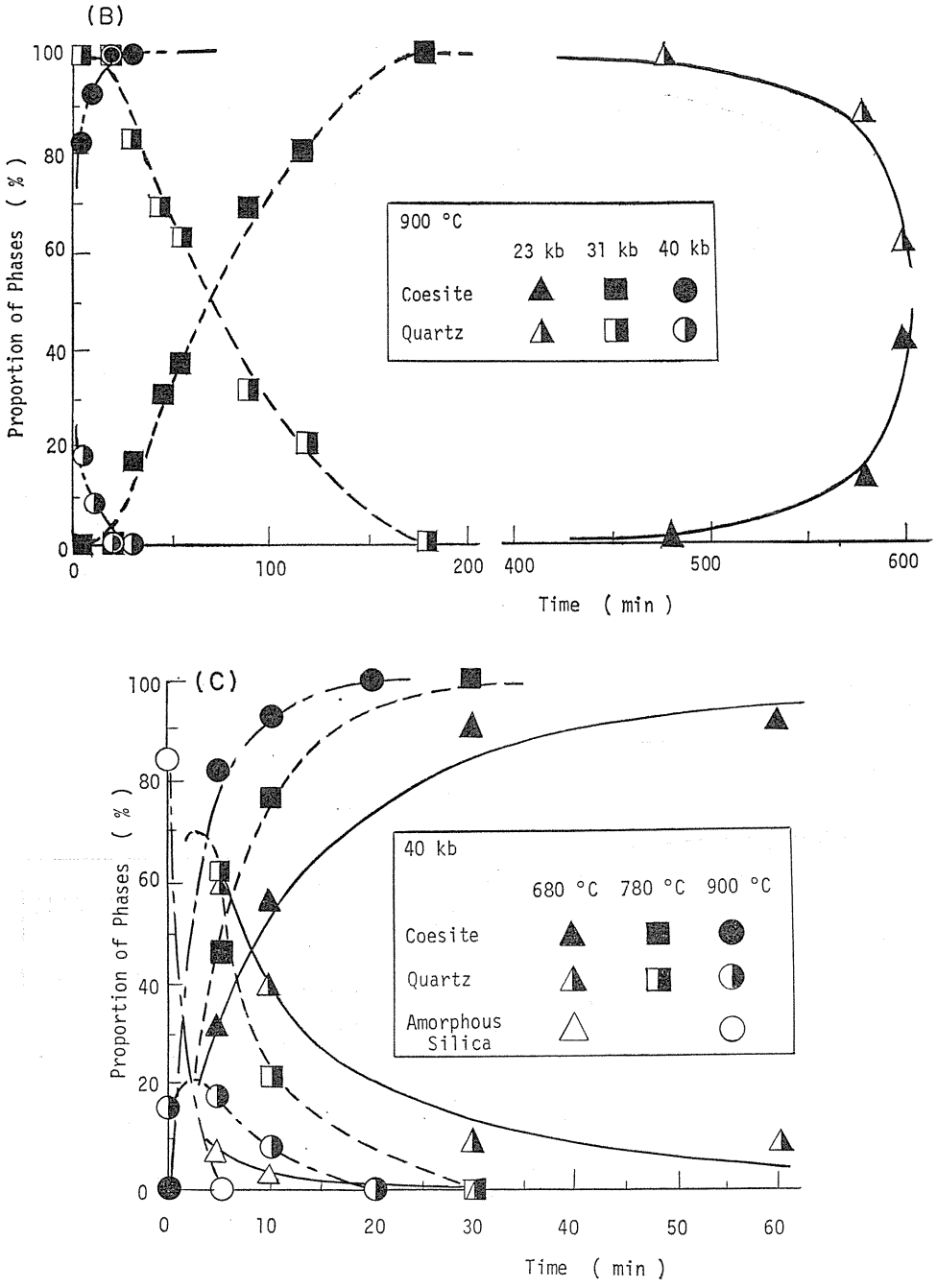

Fig. 4. 2. Variations in the proportion of starting amorphous silica, intermediate phase of metastable quartz and the equilibrium phase of coesite with heating time under various pressure-temperature conditions.
(A) : under various pressures at 550 ℃,
(B) : under various pressures at 900 ℃,
(C) : at various temperatures under 40 kbars.

These experimental results on the formation of coesite from amorphous silica show that the higher the temperature, the faster the apparent rate of formation of coesite and the larger the maximum amount of the intermediate quartz. The intermediate qnartz seems to be highly strained, since its diffraction profiles are broadened more than those of the quartz starting material, as shown in Fig. 4. 3.

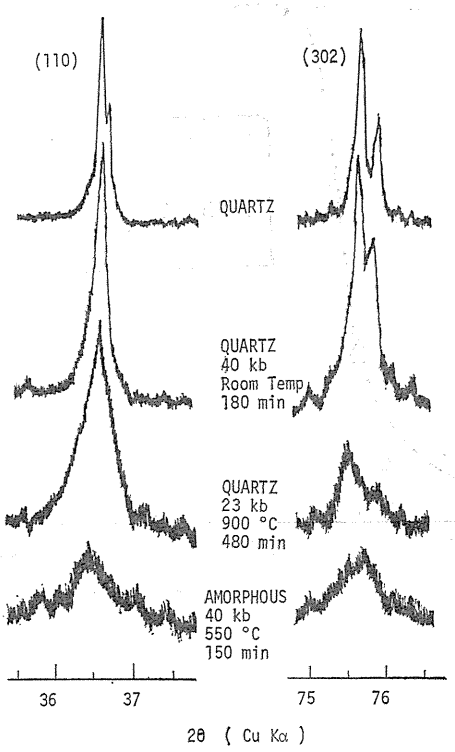

Fig. 4. 3. The diffraction profiles of (110) and (302) lines of quartz used as a starting material and quartz formed under pressure.

4. 3. 2. Crystallization Kinetics of Coesite from Quartz

In Fig. 4. 4, the variations in the amount of coesite with heating time are shown under various pressure-temperature conditions. In most samples, the only phase coexisting with coesite was quartz. The rate of coesite formation increases with temperature and pressure.

The observed diffraction profiles of quartz are also broadened, as for the strained quartz formed from amorphous silica (Fig. 4. 3). In Fig. 4. 5, the variation in the broadness (half width β) of the diffraction lines with heating time is shown as a plot of $(\beta \cos\theta)/\lambda$ vs. $(\sin\theta)/\lambda$. Under all conditions, the lattice strain ε of the quartz phase showed a maximum, which was evaluated from the slope of these plots by using Hall's equation (2. 1). This maximum occurred before the rapid increase in the amount of coesite. The correspondence between lattice strain of quartz and the amount of coesite is shown in Fig. 4. 6. At 900 ℃ under 31 kbars

pressure, the measured lattice strain was relatively small, but decreased with increasing heating time, suggesting that the maximum in strain was already passed at short time of heating. Such a high value of lattice strain was never obtained by compression at room temperature, as shown in Fig. 4. 6.

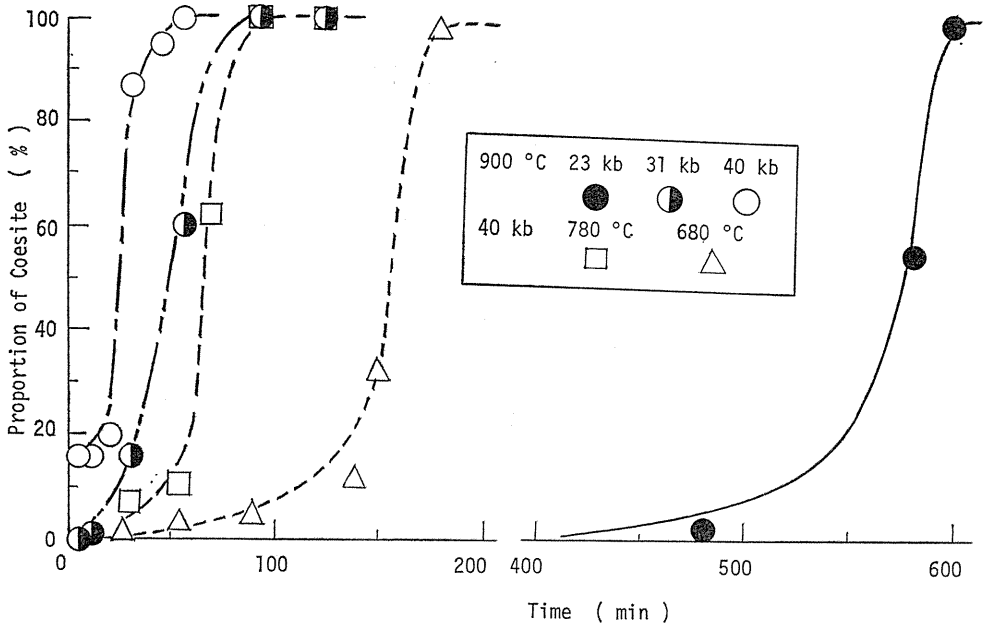

Fig. 4. 4. Variations in proportion of coesite formed from quartz under various pressures and temperatures with time.

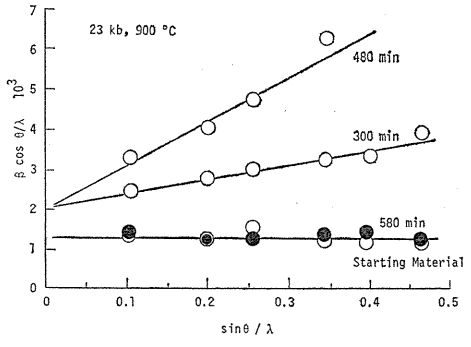

Fig. 4. 5. Relation between $(\beta \cos \theta)/\lambda$ and $(\sin \theta)/\lambda$ for quartz phase heated under 23 kbars pressure at 900℃ for various times.

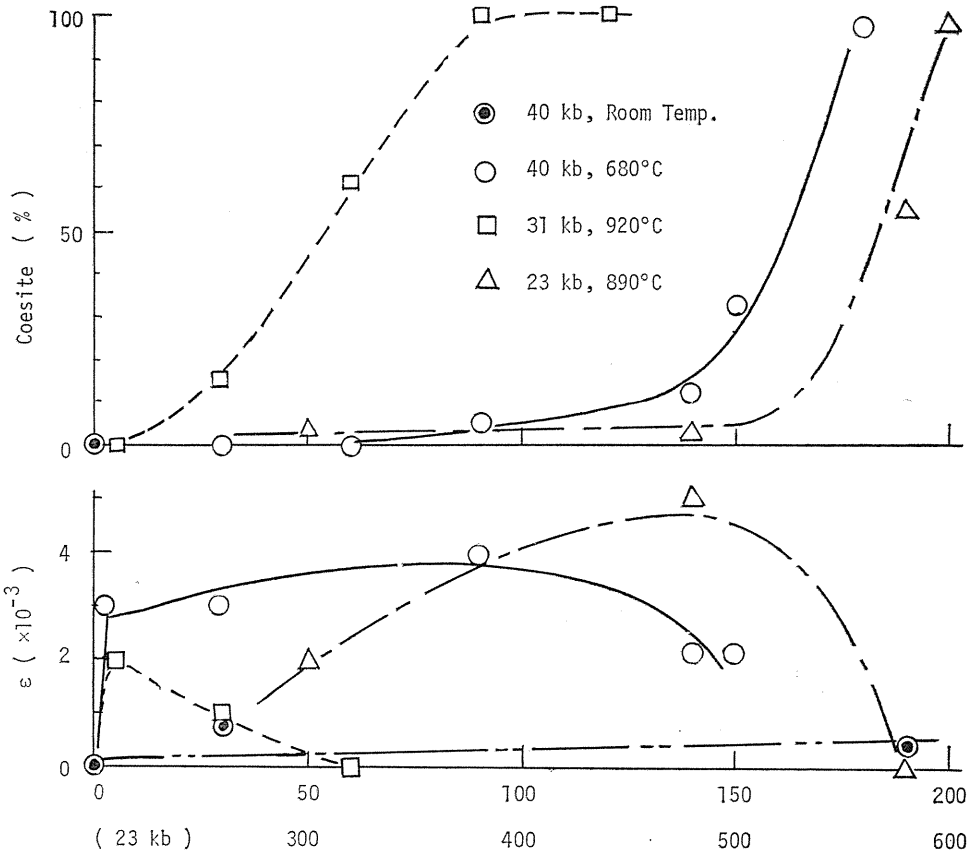

Fig. 4. 6. Correspondence between lattice strain of quartz and amount of coesite formed. The values of lattice strain induced in quartz by compression under 40 kbars at room temperature are shown for the comparison.

4. 4. Discussion

4. 4. 1. Kinetic Process of Crystallization of Coesite from Amorphous Silica

The experimental results on the formation of coesite from amorphous silica, particularly the results shown in Fig. 4. 2-A, show that the process is a consecutive one through metastable quartz which is highly strained. It can be expressed as follows:

$$\text{amorphous silica} \xrightarrow[k_A]{} \text{quartz (highly strained)} \xrightarrow[k_C]{} \text{coesite,} \tag{4.1}$$

where k_A is the rate constant for the first-step transition from amorphous silica to quartz and k_C that for the second-step transition from quartz to coesite.

All of the complicated experimental results, for example a peculiar change of the apparent rate of formation of coesite with pressure at a constant temperature 550 ℃ (Fig. 4. 2-A), are explained qualitatively by assuming the consecutive process as Eq. (4. 1) and also the dependencies of the rate constants of each step, k_A and k_C, on pressure and temperature. At 550 ℃ under 40 kbars pressure, k_A is approximately comparable to k_C and, therefore, a maximum occurs in the amount of the intermediate quartz, as for the typical consecutive rate process shown in the fundamental text books. At the same temperature and under other pressures, the rate constans are not equal with each other, and one or the other transition becomes a rate-determining step. Under 55 kbars pressure, the rate-determining step seems to be the transition from amorphous silica to the intermediate quartz, since the observed amount of quartz is only a trace. Under 31 kbars, in contrast, the other transition, *i. e.* the transition from the intermediate quartz to coesite, seems to be rate-determining, and a larger amount of quartz is found than under 40 kbars. Because the transition to coesite is retarded under pressures both higher and lower than 40 kbars, the rate constants k_A and k_C must depend very differently on pressure, the latter increasing sharply with pressure and the former having slight or no dependence on pressure. Therefore, $k_A \approx k_C$ under 40 kbars, $k_A < k_C$ under 55 kbars and $k_A > k_C$ under 31 hbars are realized.

Both rate constants also depend positively on temperature. At 40 kbars, the rate of formation of coesite and the maximum amount of quartz increase with increasing temperature (Fig. 4. 2-A and -C). Therefore, the temperature dependence of k_A seems to be stronger than that of k_C. The results at 900 ℃ under different temperatures can be explained consistently by using the same dependencies of both rate constants on pressure and temerature; the first step from amorphous silica to quartz is much more faster than at low temperatures, consequently no amorphous silica detected, and the second step from quartz to coesite shows very remarkable pressure dependence of rate constant k_C, as pointed out before at 550 ℃.

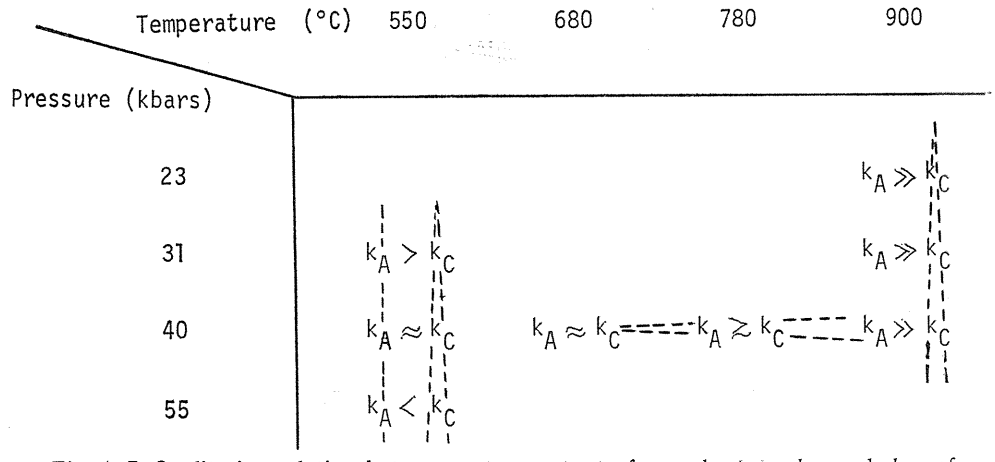

Fig. 4. 7. Qualitative relation between rate constants for each steps, k_A and k_C, of the crystallization of coesite from amorphous silica under various pressure-temperatuer conditions. The expected dependencies of each costants on pressure and temperature are also shown by broken lines.

In Fig. 4. 7, the mutual relation between the rate constants of each step, k_A and k_C, and the changes of both rate constants with temperature and pressure are illustrated for the temperatures and pressures examined in the present work.

4. 4. 2. Kinetic Process of Crystallization of Coesite from Quartz

The experimental results show that the starting quartz must be strained before transforming to coesite. Similar to Eq. (4. 1), a consecutive rate process can be written :

$$\text{quartz} \xrightarrow[k_Q]{} \text{quartz (highly strained)} \xrightarrow[k_C]{} \text{coesite}, \tag{4.2}$$

where k_Q and k_C are the constants for respective transitions. The rate constant k_C is expected to have the same pressure and temperature dependencies as k_C in the case of starting from amorphous silica (Eq. (4. 1)). The rate constant k_Q seems to increase with increasing temperature. The pressure dependence of k_Q is believed to be very small and similar to that described for amorphous silica; it may even be negative, because the increase in strain involves a decrease in density.

Further quantitative discussion on the rate of formation of coesite from quartz is unwarranted because only a general assessment of lattice strain in the quartz phase can be made for this process from the present results.

4. 4. 3. Effect of Starting Material on Rate of Crystallization

At 900 ℃, the apparent rate of formation of coesite from quartz is faster than that from amorphous silica under 23 and 31 kbars pressure, but slower under 40 kbars (Figs. 4. 2-B and 4. 4). Under 40 kbars, amorphous silica converts faster to coesite than quartz does at all temperatures examined, and the rate of formation of coesite increases with incresing temperature. The results can be explained by the relation between the rate constants k_A and k_Q in the kinetic processes of Eqs. (4. 1) and (4. 2), assuming that k_C is the same in both consecutive processes. Under 23 and 31 kbars, k_A seems to be smaller than k_Q, and under 40 kbars, k_A is larger than k_Q. This inversion in k_A and k_Q can occur because of the different pressure dependencies of k_A and k_Q; k_A seems not to depend on pressure, but the pressure dependency of k_Q may be negative, as mentioned above. Under 40 kbars, $k_A > k_Q$ held at all temperatures examined.

The difference in the rates of formation of coesite from amorphous silica and quartz can be related to the equilibrium phase boundary between quartz and coesite. In the region near the boundary, i. e. at 900 ℃ under 23 and 31 kbars (points 1 and 2 in Fig. 4. 1), the observed rate of formation from quartz is faster than that from amorphous silica, whereas in the region far from the boundary, e. g. at 900°, 780°, 680° and 550 ℃ under 40 kbars (points 3 to 6 in Fig. 4. 1), amorphous silica converts to coesite faster than quartz.

Chapter 5. Morphological Development of Coesite

5. 1. Introduction

Coes (1953) synthesized coesite by reacting dry sodium metasilicate with am-

monium phosphate at 700 ℃ under 40 kbars pressure for 16 h, of which crystals were discrete pseudohexagonal platelets. Boyd & England (1960) obtained hexagonal flakes and euhedral lath-shaped crystals of coesite from silicic acid at 700 ℃ under 24 kbars for 2 h. Sclar et al. (1962) reported simple contact twins with twin plane of (021) in addition to hexagonal platelets and lath-shaped crystals of coesite by using hydrated silica gel as a starting material. The morphological development of coesite has been discussed in the relation to various factors depending on the type of high-pressure apparatus (Sclar et al., 1962). However, it must be iufluenced by the kind of reactants used, as much as by the over-all pressure-temperature conditions for the transition to coesite and for growth of coesite. We found that coesite crystallized from amorphous silica by a consecutive process throgh intermediate phase of metastable quartz, and that the rates of each elemental step in the consecutive process and also their mutual relation depend strongly on the pressure-temperature condition.

In the present chapter, the development of the characteristic morphology of coesite crystals formed under anhydrous condition was investigated. The morphological development of metastable quartz was also followed and its controlling effect on the morphology of coesite was discussed.

5. 2. Experimental

The starting materials used were amorphous silica, prepared by hydrolysis of $SiCl_4$ ("amorphous silica A")' and natural quartzite, "quartz A", as described in Chapter 2.

The cell arrangement of the girdle-type high-pressure apparatus was shown in Fig. 2. 1. The crystallization was carried out under the pressure of 20 ~ 55 kbars at the temperature of 550 ~ 1300 ℃ for various periods in the absence of water. The crystals formed were observed under an optical microscope by using thin sections.

5. 3. Results and Discussion

5. 3. 1. Morphology of Crystals formed from Amorphous Silica

In Figs. 5. 1 and 5. 2, the micrographs of crystals of metastable quartz and stable coesite formed from amorphous silica under 31 kbars pressure at 900 ℃ for different times (30, 60 and 180 min) are represented. As shown in the preceding chapter, amorphous silica converted completely to quartz and coesite before 30 min (Fig. 4. 2-B) : the proportion of quartz is 80 % after 30 min, 60 % after 60 min and only a trace after 180 min. In the samples heated for 30 and 60 min, coesite crystallizes in the matrix of fine-grained quartz (Figs. 5. 1 and 5. 2-A ~ -D). The particles of metastable quartz are roughly 7 ~ 8 μm in size, of which grain boundaries are irregular and indistinct, and appreciable grain growth is not observed with increasing heating time. These fine-grained quartz is likely to be detected as highly-strained intermediate quartz in the preceding kinetic studies. On the other hand, the coesite crystals grow, seeming at the expense of fine-grained metastable quartz, and change their habits with increasing time. The crystals of coesite observed often in the samples are pseudohexagonal platelets (Fig. 5. 1 -E and -F) and needle-like lath-shaped ones (Fig. 5. 1-A ~ -D), the latter being more abundant than the former. The pseudohexagonal platelets of coesite with the size of 0. 1 ~ 0. 2 mm are found mostly in the samples heated for less than 60 min, of which

degree of elongation (ratio of length to breadth of the crystal) is 1.2 ~ 1.3. In the samples heated for long period, only lath-shaped crystals which elongate along the crystallographic c-axis are found. After 30 min, they are 0.1 ~ 0.2 mm in size of which degree of elongtion is about 4 ~ 9. After 60 min, their size grows a little to 0.1 ~ 0.3 mm, but a variety of crystals are found, from the bulky to thin lath-shaped ones, as wide range of degree of elongation (ca. 2 ~ 11) indicates. After 180 min, the crystals grow to 0.3 ~ 0.6 mm and have homogeneous shape (the degree of elongation is in narrow range of 3 ~ 5). In these lath-shaped crystals, the subconcoidal fractures (Sclar et al., 1962) normal to the c-axis are often

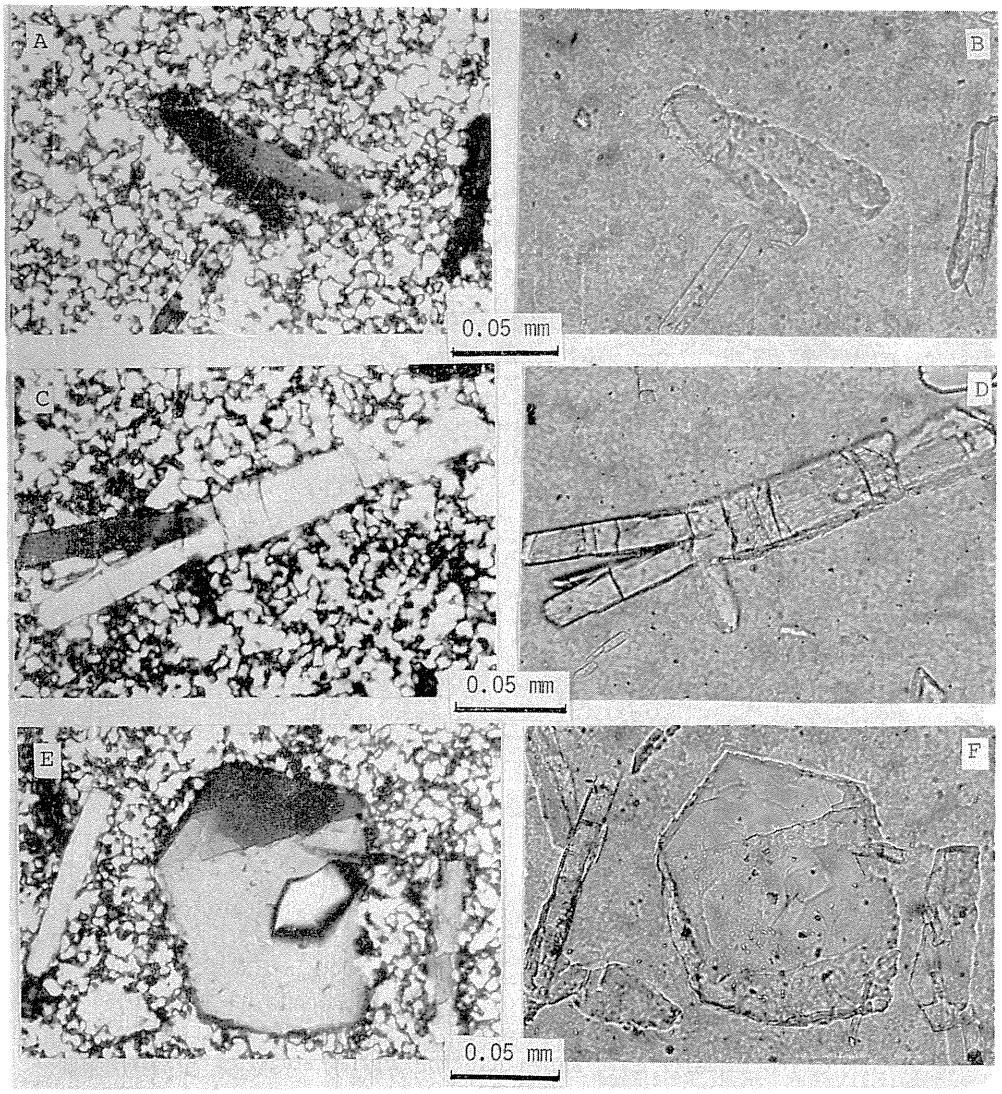

Fig. 5. 1. Micrographs of coesite crystals formed from amorphous silica under 31 kbars at 900°C for 30 min. Both micrographs under open nicol and crossed nicols are shown at the same regions.

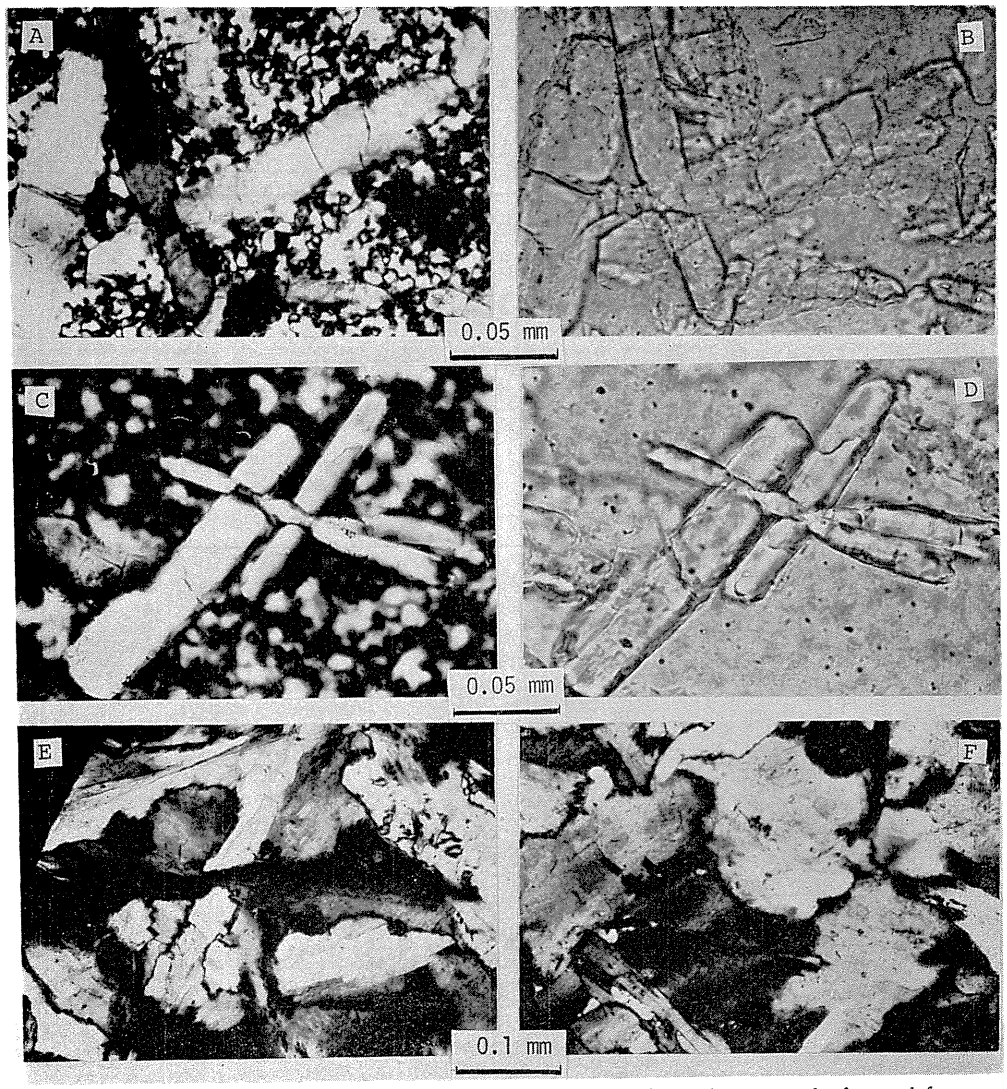

Fig. 5. 2. Micrographs under open and crossed nicols of coesite crystals formed from amorphous silica under 31 kbars at 900 ℃ for 60 min (A ~ D) and for 180 min (E and F).

observed (Fig. 5. 1-C and -D, Fig. 5. 2-A and -B). The penetration twins as shown in Fig. 5. 2-E are also found. The early stage of the formation of these twins, which will be discussed in Chapter 7, is likely to be seen in Fig. 5. 2-C and -D.

Crystallization process of coesite from metastable quartz has been observed on the samples heated under 23 kbars pressure at 900 ℃, where the crystallization rate of coesite from quartz is so slow that the initial stage of crystallization is able to be observed (Fig. 4. 2-B). Representative micrographs are shown in Fig. 5. 3. After 300 min, large spherulitic aggregates of quartz crystals (ca. 0. 3 mm in size) are found in the matrix of fine-grained quartz (Fig. 5. 3-A and -B). In the

same sample, the dendritic crystals of coesite which are supposed to be grown from the aggregates of quartz are also observed (Fig. 5. 3-C and -D). The dendrites of coesite elongate along the c-axis and suggest the rapid growth at the expence of quartz matrix. The lath-shaped and even plate-like crystals of coesite are found the more abundant in the samples heated for the longer time (Fig. 5. 3-C ~ -F). Some of them have well-defined crystal habit, but some are still obscure. These observations under microscope agree well with the results of the kinetic studies (Fig. 4. 2-B) ; amorphous silica transforms completely to intermediate quartz in very short time and coesite appears abruptly after a long induction period.

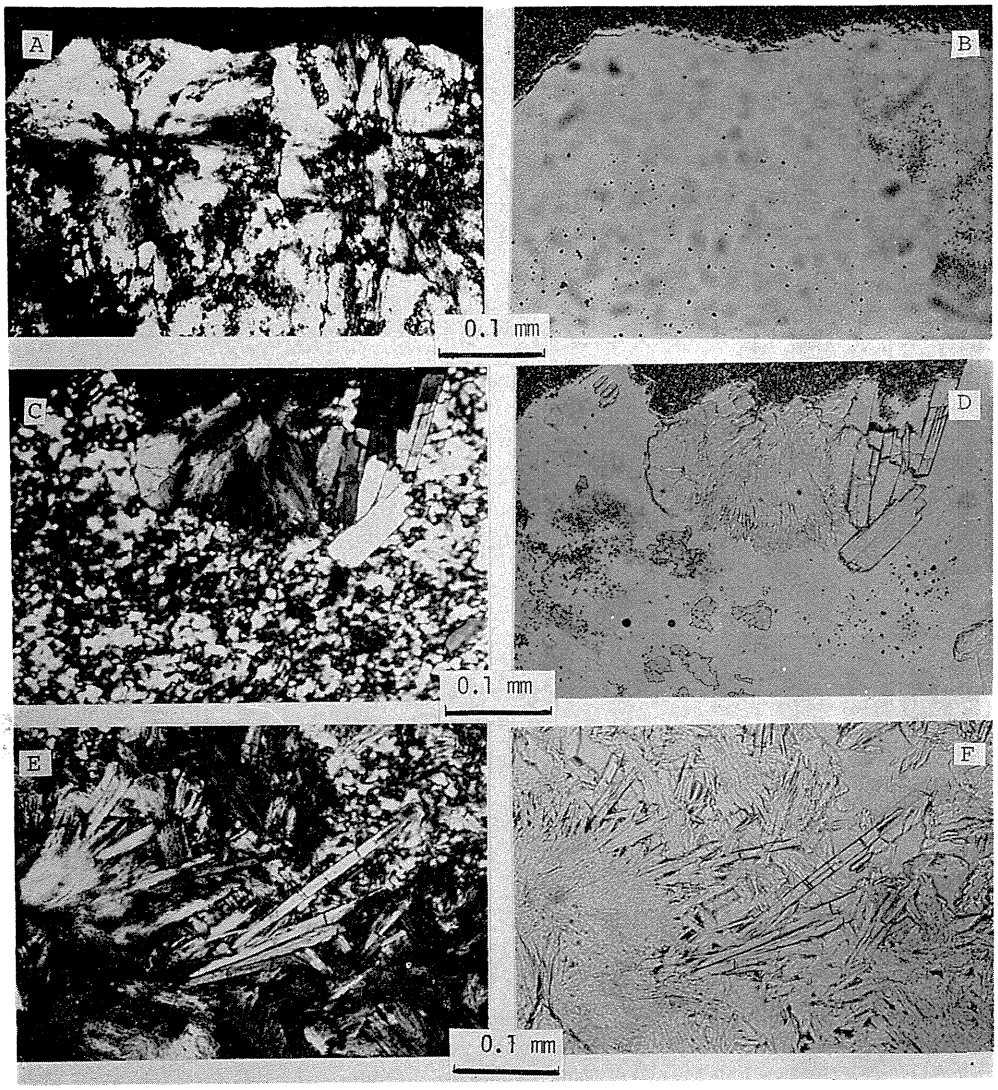

Fig. 5. 3. Micrographs under open and crossed nicols of quartz and coesite crystals formed from amorphous silica under 23 kbars at 900℃ for 300 min (A ~ D) and for 600 min (E and F).

In Fig. 5. 4, the crystallization process of coesite under various conditions are shown by presenting the crystal morphology. The spherulitic aggregates of metastable quartz become small as the applied pressure increases; ca. 0.2 mm under 31 kbars (Fig. 5. 4-A and -B) and less than 0.05 mm under 55 kbars (Fig. 5. 4-D). Coesite crystals with the size of ca. 0.02 mm long are found to crystallize in needle-like shape at the center of the spherulites of quartz (Fig. 5.4-A). The

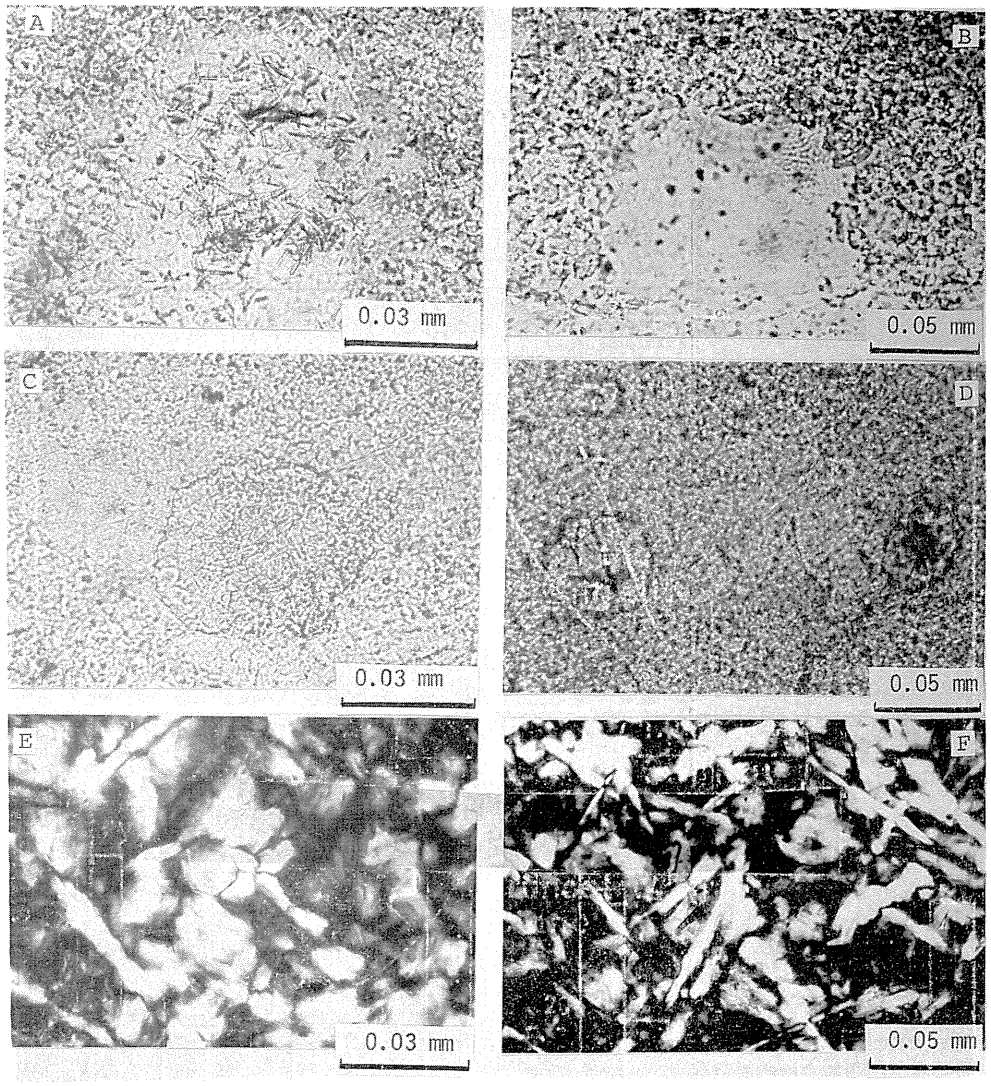

Fig. 5. 4. Micrographs of quartz and coesite crystals formed from amorphous silica under various conditions.

A and B: 550 ℃, 31 kbars, 180 min,
C: 550 ℃, 40 kbars, 150 min,
D: 550 ℃, 55 kbars, 210 min,
E and F: 900 ℃, 40 kbars, 60 min.

similar observation has been reported on the reverse transition of coesite to quartz (Livshits et al., 1972). Under 40 kbars at 900 ℃, coesite crystallizes in lath-shape with the size of about 0.1 mm long (Fig. 5. 4-E and -F). The crystal size of coesite decreases with increasing pressure and with decreasing temperature. In the preceding chapter, we knew the mutual relation between the rate constants k_A and k_C for each elemental steps of the consecutive process from amorphous silica to coesite from the quantification of the phases (amorphous silica, intermediate quartz and coesite); $k_A > k_C$ under 31 kbars at 550 ℃, $k_A \approx k_C$ under 40 kbars and $k_A < k_C$ under 55 kbars (Fig. 4.7). The crystallization of coesite in spherulitic aggregates of metastable quartz observed under optical microscope agrees with the relation between k_A and k_C; under 31 kbars the crystallization of coesite is retarded, but under 55 kbars occurs so fast that the spherulitic aggregates mostly consist of fine crystals of coesite are often found.

5. 3. 2. Morphology of Crystals formed from Quartz

In Figs. 5. 5 and 5. 6, some micrographs of the samples heated under various conditions are shown. The crystals of coesite obtained from quartz are evidently smaller than those from amorphous silica, but scheme of the crystallization process and effect of pressure-temperature condition on the size of coesite are not different from starting materials.

Under 20 kbars at 870 ℃ after 600 min, the needle-like crystals with lath-shape of 0.03 ~ 0.1 mm long and also the pseudohexagonal platelet crystals are observed in the matrix of metastable quartz (Fig. 5. 5-A ~ -D). Some of the lath-shaped crystals of coesite contain the characteristic subconcoindal fractures, which have also been observed in those formed from amorphous silica. The coesite crystals are 0.02 ~ 0.1 mm in size under 23 kbars at 900 ℃ after 580 min, being a little smaller than under 20 kbars (Fig. 5. 5-E and -F). Under 31 kbars, most of the coesite crystals are lath-shaped and 0.15 ~ 0.05 mm long (Fig. 5. 6-A ~ -C). These remarkable decrease in size of coesite crystals is probably due to the frequent nucleation of coesite which occurs abruptly under high pressures. The subconcoidal fractures are less abundant to be found in the crystals formed under higher pressure. With increasing heating time, the growth along the c-axis of coesite crystals are not appreciable, but bulky crystals are often observed and the penetration twins also occur at high temperatures (Fig, 5. 6-D).

At early stage of crystallization, spherulitic aggregates of metastable quartz are observed (Fig, 5. 6-A) as in the samples prepared from amorphous silica described above. The crystallization of coesite seems to be delayed in the aggregates than in the matrix of fine grains of metastable quartz. After long time heating, the aggregates of quartz tend to become small and disappear.

The observed difference in morphological development of coesite crystals formed from amorphous silica and quartz is probably due to the difference in shear exerted on the sample, as well as the difference in aggregation of metastable quartz and nucleation of coesite. Preferential growth along the c-axis under shear will be discussed in Chapter 7.

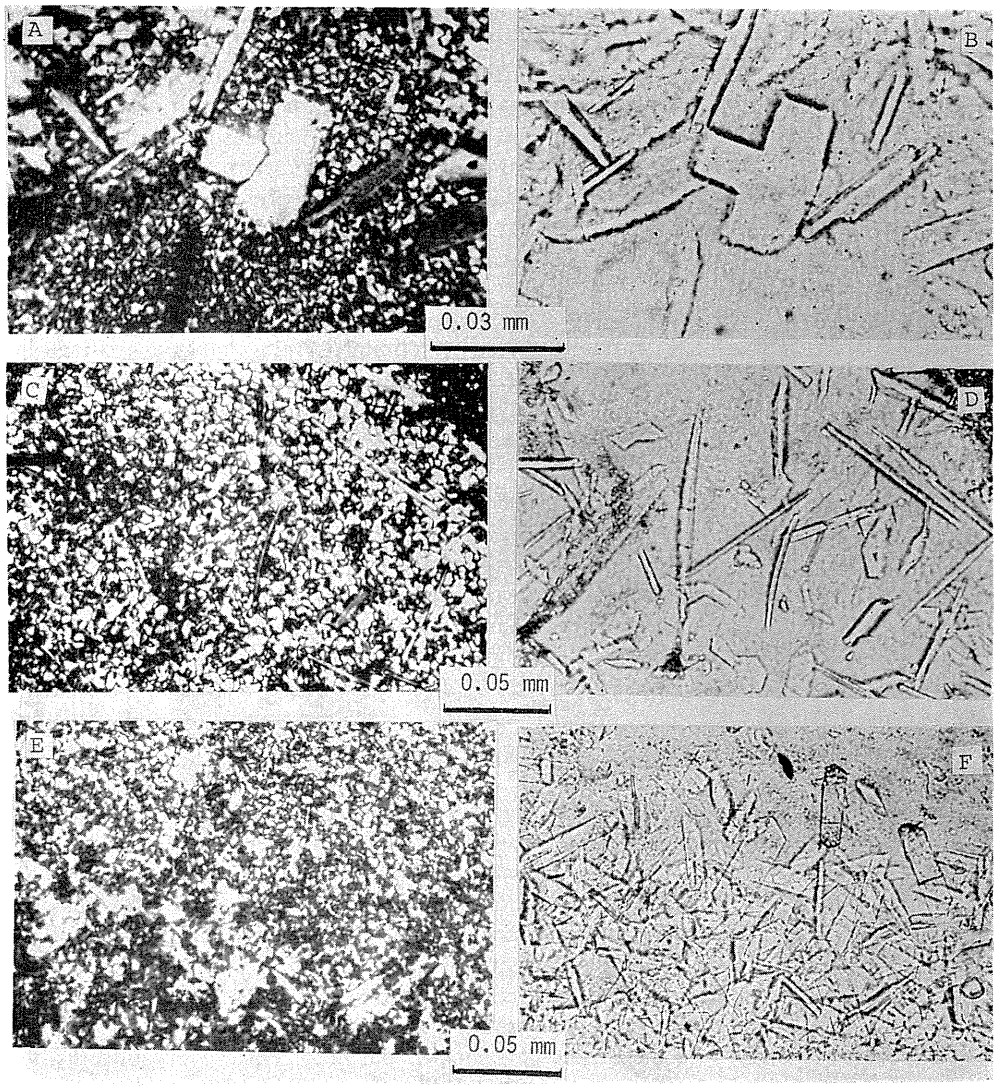

Fig. 5. 5. Micrographs under open and crossed nicols of crystals formed from quartz under 20 kbars at 870 ℃ for 600 min (A ~ D) and under 23 kbars 900 ℃ for 580 min (E and F).

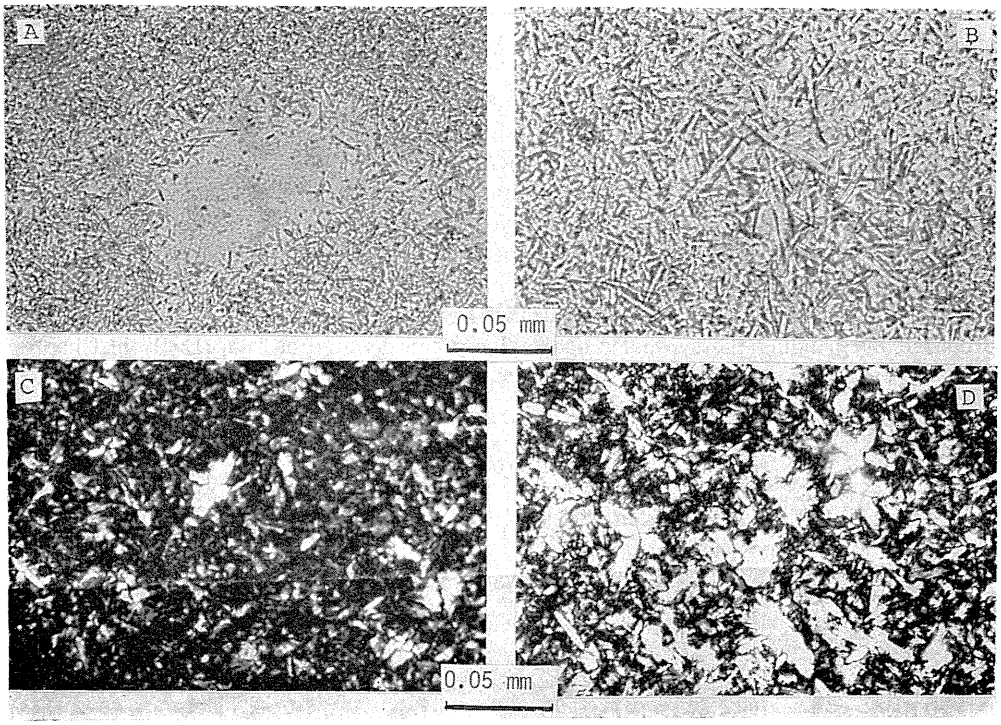

Fig. 5. 6. Micrographs under open and crossed nicols of crystals formed from quartz under 31 kbars at 900℃ for 30 min (A), 60 min (B) and 120 min (C) and at 1300℃ for 60 min (D).

Chapter 6. Crystallization of Coesite from Various Starting Materials in the Presence of Water

6. 1. Introduction

In the preceding chapters, the crystallization of coesite from amorphous silica was found to be a consecutive rate process through intermediate phase of metastable quartz under various pressure-temperature conditions. The morphology of crystals formed during crystallization process was studied: the formation of characteristic spherulitic aggregates of metastable quartz and the formation of penetration twins of coesite were observed. The morphology of stable phase of coesite was discussed in the relation to that of intermediate phase of quartz.

On the other hand, water has a very important role in various phase transitions, as well as in the crystallization and crystal growth of oxides. Many reports have dealt with the effect of water on the transitions of silica (Kracek, 1953; Boyd & England, 1960; Zeto et al., 1962; Wagstaff et al., 1964; Wagstaff & Richards, 1966; Uhlmann et al., 1966).

In the present chapter, the effect of water on the crystallization process of coesite was studied in detail, paying attention to crystallization kinetics and crystal morphology of quartz and coesite, by using various starting materials.

6. 2. Experimetal

The cell arrangements of the girdle-type high-pressure apparatus shown in Figs. 2. 1 and 2. 2 were used. The formation of coesite was performed at the temperature range of 100° to 700°C under the pressure of 30 ~ 90 kbars, mostly under 30 kbars, for various durations up to 96 h either with or without water. Amount of water added into the sample was 4, 10 and 16 wt%.

The starting materials used were amorphous silica, silica glass and synthetic quartz. The amorphous silica was prepared by hydrolysis of silicon ethoxide and described as "amorphous silica B" in Chapter 2. It has particle size of 0. 1 ~ 10 μm. The silica glass was a commercial one which was ground to the particle size of 0. 5 ~ 1. 0 μm. The quartz powder with particle size of 0. 5 ~ 1. 0 μm was prepared by grinding the synthetic quartz lump and denoted as "quartz B" in Chapter 2.

6. 3. Results

6. 3. 1. Crystallization Kinetics of Coesite from Amorphous Silica

In Fig. 6. 1, the variations in the proportion of amorphous silica, intermediate phase of quartz and equilibrium phase of coesite with heating time with 10 wt% water are compared with those without water at 450 ℃ under 30 kbars pressure.

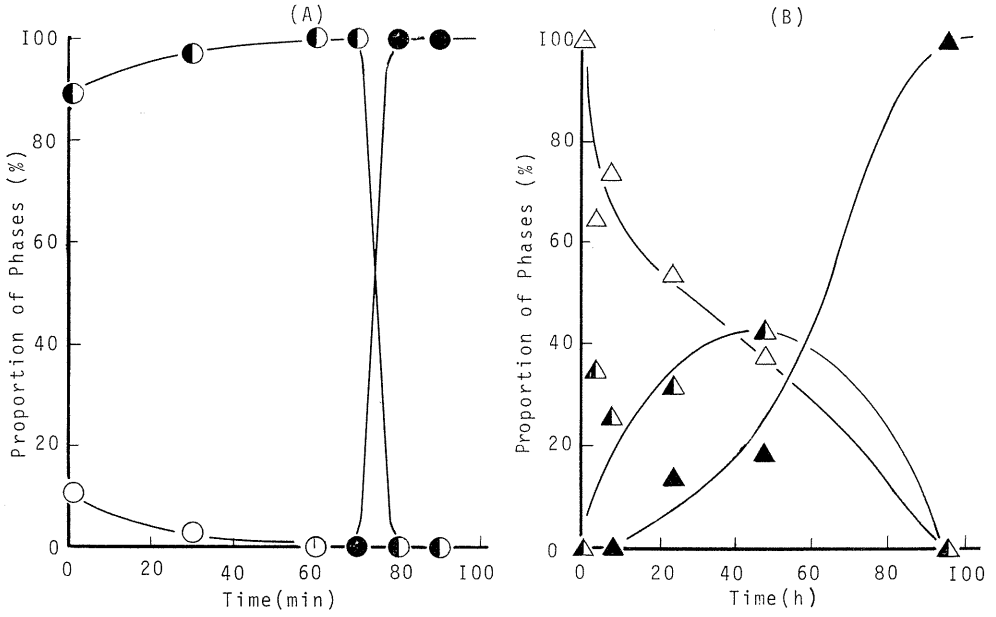

Fig. 6. 1. Variations with time in proportion of amorphous silica (open marks), quartz (half-filled) and coesite (filled) under 30 kbars at 450℃.
A: with 10 wt% water, B: without water.

The rate process in the case without water (Fig. 6. 1-B) is typically consecutive, with $k_A \approx k_C$, as shown in previous section. The proportion of intermediate quartz phase goes through a maximum at about 48 h. After passing the maximum in the

amount of quartz, coesite increases quickly. In the presence of 10 wt% water (Fig. 6. 1-A), however, most of the amorphous silica converts to intermediate quartz phase within a few minutes, and the quartz then transforms rapidly to coesite after 70 to 80 min. The transition from amorphous silica to coesite in the presence of water appears also to be a consecutive process with $k_A \gg k_C$. Comparing of the kinetics observed in the presence and absence of water and noting that the units of the abscissas in two figures are very much different, each steps in the consecutive process are found to be accelerated by water, particularly the first step does.

The amount of water added has also remarkable effect on the formation rate of coesite. In Fig. 6. 2, the variations with time in proportion of intermediate quartz and coesite formed under 30 kbars pressure at 600 ℃ are shown in the presence of 4 wt% and 16 wt% water, and without water (note the difference in unit of abscissas). At 600 ℃, the amorphous silica apparently converts to intermediate quartz very quickly and therefore only quartz and coesite are identified in the sample after the heat-treatments. As the water content increases, the rate of transition of quartz to coesite also increases. We must note that the presence of only 4 wt% of water remarkably reduces the heating time for 100 % transition of quartz to coesite.

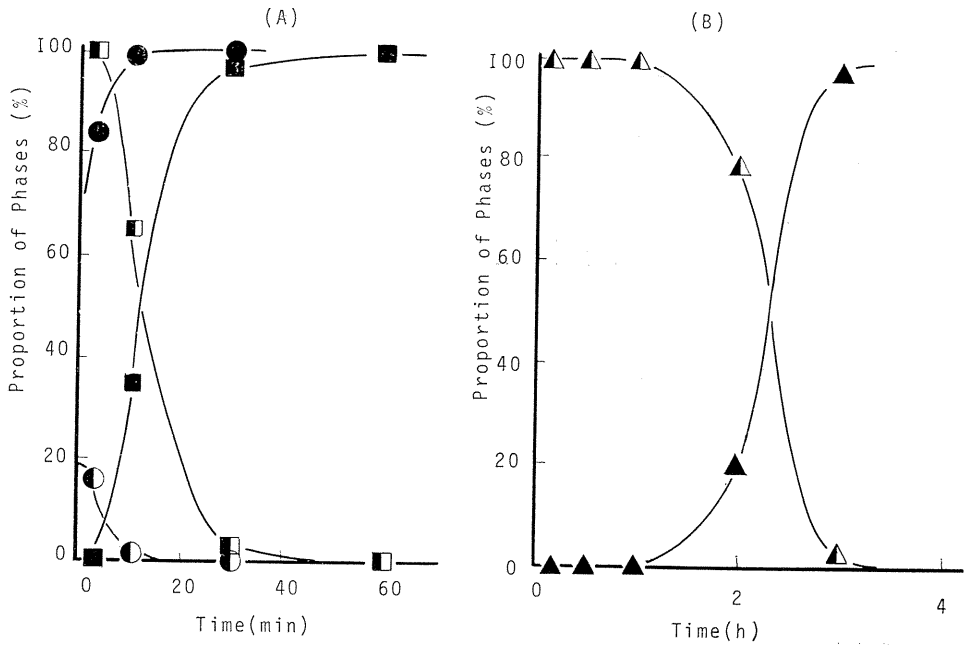

Fig. 6. 2. Variations with time in proportion of quartz (half-filled marks) and coesite (filled) under 30 kbars at 600 ℃.
A: with 4 wt% water (squares) and 16 wt% water (circles),
B: without water.

Raising the temperature not only accelerates both steps of the consecutive transition but also changes the relation between the rate constants for both steps, i. e. $k_A \approx k_C$ at 450 ℃ and $k_A \gg k_C$ above 600 ℃ without water. The same results

has been described in Chapter 4. The addition of water is known to be the same effect as increasing the temperature i. e. $k_A \gg k_C$ even at low temperature as 450℃ with 10 wt% water.

In order to show the effect of water on formation rate of coesite, the amount of coesite formed is plotted as a function of heating temperature under various pressures (Fig. 6. 3). The heating time was kept constant as 1 h. All curves obtained under different pressures with or without water are very similar in shape and show how abrupt the transition to coesite occurs at a certain temperature. This temperature becomes the lower by the compression under the higher pressure. It is also noteworthy that the existence of 10 wt% water lowers the temperature, at which the transition to coesite occurs abruptly, by roughly 200℃ at least under the pressure examined.

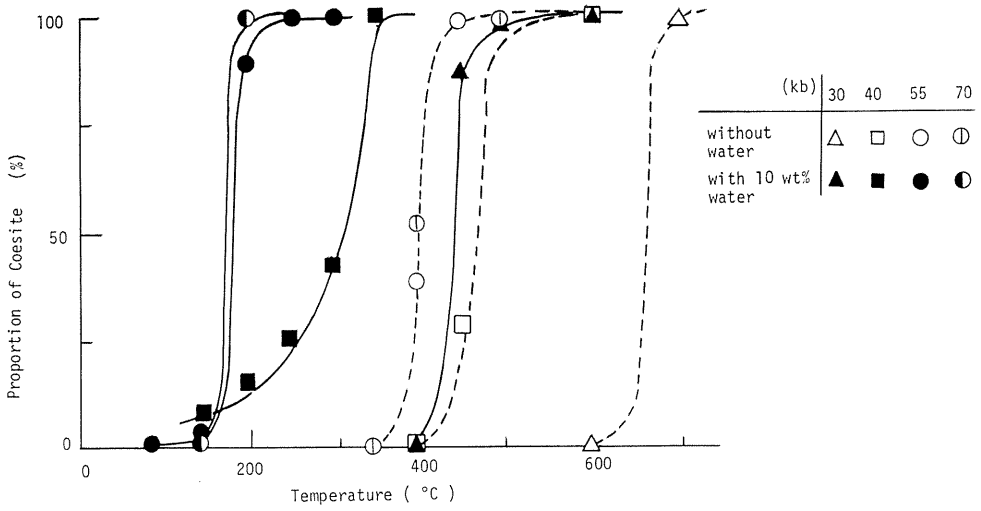

Fig. 6. 3. The amount of coesite formed under various pressures and temperatures for 1 h with 10 wt% water and without water.

6. 3. 2. Crystal Morphology of Quartz and Coesite formed from Amorphous Silica

The effect of water addition was seen not only from kinetics but also from morphology of intermediate phase of metastable quartz and equilibrium phase of coesite. In Fig. 6. 4 and 6. 5, the micrographs of the samples heated under 30 kbars pressure at 450° and 600 °C for various times are shown in order to exhibite the crystal morphology of quartz and coesite phases.

Without water, metastable phase of quartz crystallized into spherulitic aggregates with the apparent size of 50 μm in maximum after heating at 450℃ for 4 h; coesite phase being not yet detected in X-ray powder pattern (Fig. 6. 1-B) and under microscope. These spherulites of quartz were formed in the matrix of unchanged amorphous phase and consisted of fine crystals with the size of 0. 5 ～ 1. 0 μm, of which c-axes oriented radially . The size of the spherulites increased with the increase of heating time, up to 300 μm after 48 h.

In the center of the spherulites, where the radial orientation of quartz crystals

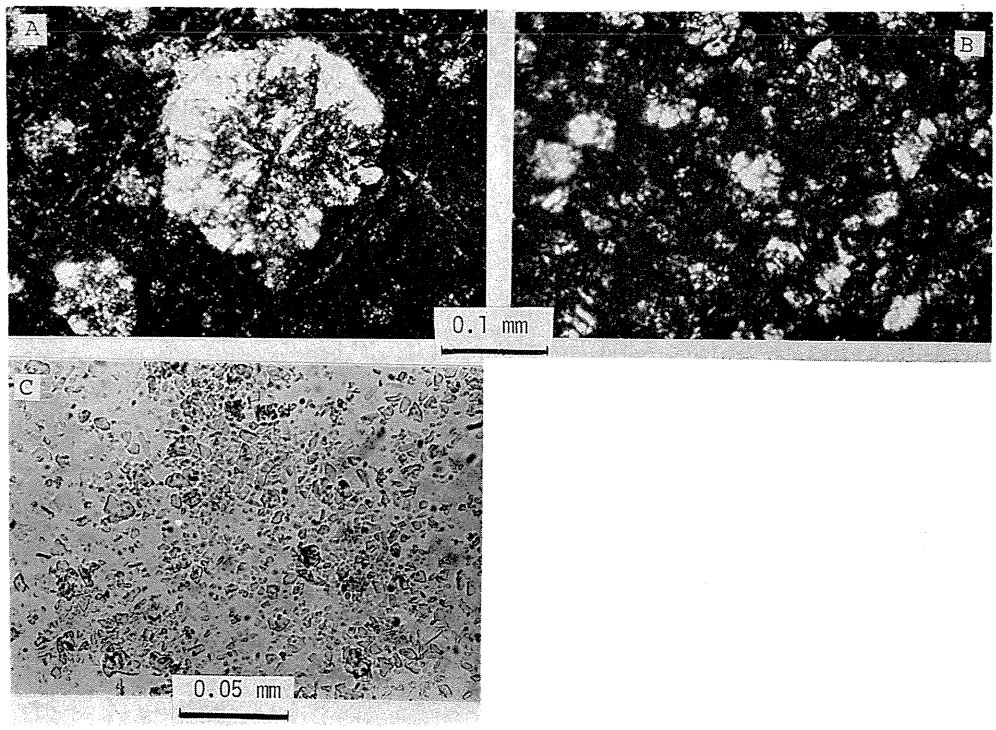

Fig. 6. 4. Micrographs of crystals formed from amorphous silica under 30 kbars at 450 ℃.
A: 48 h without water (under crossed nicols),
B: 1 h with 10 wt% water (under crossed nicols),
C: 80 min with 10 wt% water (under open nicol).

collapsed, needle-like crystals of coesite with the size of 20 ~ 50 μm were often found (Fig. 6. 4-A). After heating at 96 h quartz completely transformed to coesite, but the size of its crystals did not show any detectable increase.

In the existence of 10 wt% water, on the other hand, most of the starting amorphous silica was converted to metastable quartz within a few minutes, as shown in Fig. 6. 1-A, of which crystals were discrete in the size of 0. 02 ~ 0. 03 μm. The aggregtes of quartz crystals were also found in the matrix of fine crystals. After 60 min, single phase of metastable quartz was obtained (Fig. 6. 1-A) and its crystal size increased up to 0. 05 ~ 0. 06 μm (Fig. 6. 4-B). After 80 min, quartz transformed rapidly to coesite, of which crystals grew to 2 ~ 5 μm (Fig. 6. 4-C).

The similar effect of water on crystal morphology was observed during crystallization process at 600 ℃ under 30 kbars (Fig. 6. 5). Without water, amorphous silica completely transformed within 10 minutes (Fig. 6. 2-B) to sintered quartz and the size of single crystal region was 1 ~ 3 μm (Fig. 6. 5-A). In this case, the formation of metastable quartz is rather fast and the crystals sintered each other. This may be why we found only few spherulitic aggregates of quartz crystals at 600 ℃, in contrast with at 450 ℃ (Fig. 6. 4-A). After heating for 60 min, the lath-shaped and needle-like crystals of coesite with the size of about 70 μm were developed in quartz matrix (Fig. 6. 5-B). The coesite crystals occurred mostly at

grain boundaries of metastable quartz crystals, and they grew along the c-axis. After 3 h, single phase of coesite was obtained. Most of the crystals were in lath-shape and 100 ~ 300 μm in size. They showed undulatory extinction under microscope, suggesting the existence of strain in the crystals. The penetration twins of coesite crystals were often observed, on which we will discuss in the following chapter.

In the existence of 4 wt% water, amorphous silica crystallized completely to metastable quartz after only 3 minutes (Fig. 6. 2-A). In this case, many spherulitic aggregates of quartz crystals were also observed in the matrix of the fine crystals of quartz with the size of 0.5 ~ 1.0 μm (Fig. 6. 5-C). After 10 min, however, the spherulitic aggregates disappeared. The granular crystals and penetration twins of coesite were found in the matrix of fine crystals of quartz (Fig. 6. 5-D). After 60 min, the number of twins decreased and the granular crystals of coesite with the size of 20 ~ 50 μm were formed.

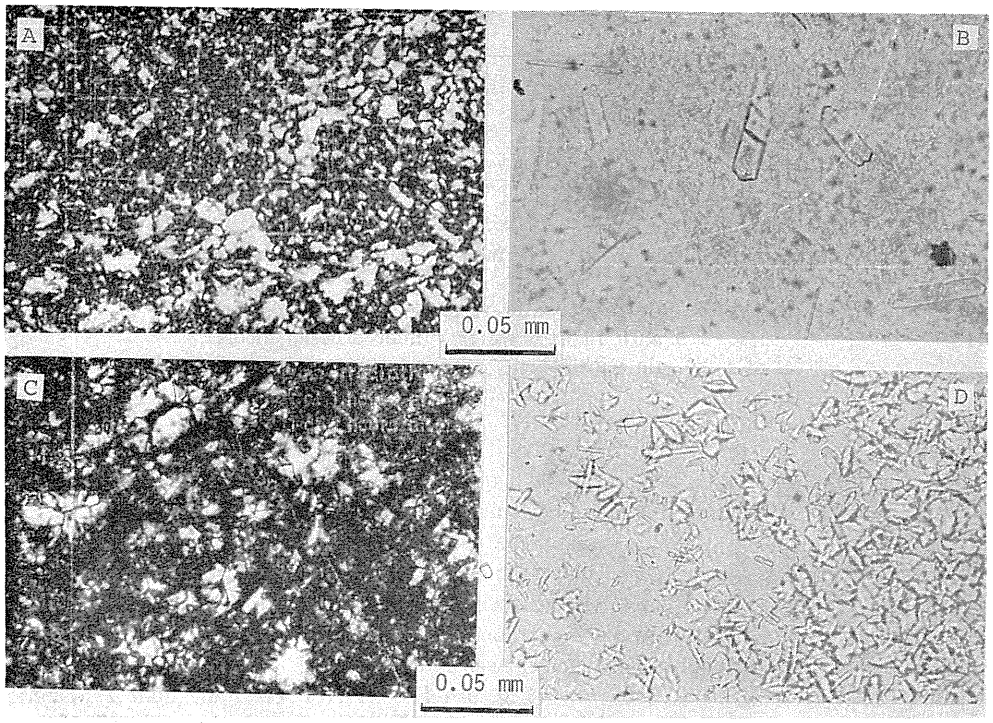

Fig. 6. 5. Micrographs of crystals formed from amorphous silica under 30 kbars at 600℃.
A: quartz aggregates, after 10 min without water (under crossed nicols),
B: Lath-shaped and needle-like coesite crystals, after 60 min without water (under open nicol),
C: quartz aggregates, after 3 min with 4 wt% water (under crossed nicols),
D: penetration twins and granular crystals of coesite, after 10 min with 4 wt% water (under open nicol).

In the existence of relatively large amount of water (16 wt%), both steps of the consecutive process from amorphous silica to coesite were so accelerated that only the morphology of coesite crystals was able to be discussed. The metastable quartz formed in very short time of heating transformed completely to coesite within 10 minutes (Fig. 6. 2-A). The spherulitic aggregates of quartz crystals and also penetration twins of coesite were hardly observed. The granular crystals of coesite grew with the increase in heating time. After 3 h, the coesite crystals as large as 100 μm were found, which were transparent and showed clear extinction.

The observation by scanning electron microscope (SEM) was carried out on some samples and the results on the sizes and morphology of crystals, which were consistent with the results obtained by polarizing microscope, were obtained. In Fig. 6. 6, SEM micrographs of metastable phase of quartz formed without water and with 16 wt% water are compared. Without water, the crystals of metastable quartz sinter and their size are rather homogeneous in 1 $\sim$ 3 μm. In the existence of water, on the other hand, the crystals of quartz are discrete and small in size (0.5 $\sim$ 1.0 μm) and relatively large crystals of coesite with the size of 5 $\sim$ 10 μm are observed.

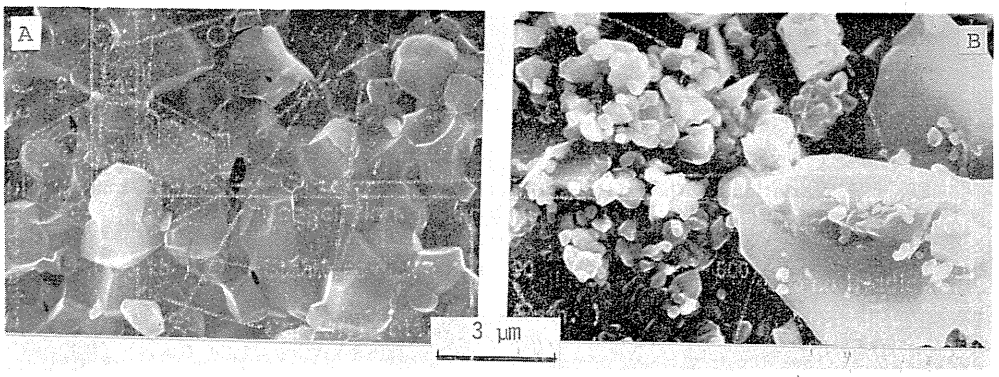

Fig. 6. 6. SEM micrographs of the crystals formed from amorphous silica under 30 kbars at 600 ℃.
A: without water for 1 h,
B: with 16 wt% water for 3 min.

6. 3. 3. Crystallization Kinetics of Coesite from Silica Glass and Crystal Morphology

Without water, silica glass remained in amorphous state even after 96 h at 450 ℃ under 30 kbars pressure and no crystallization was detected on the X-ray powder pattern. At 600 ℃ under 30 kbars, the consecutive kinetic process of crystallization of coesite through intermediate quartz was observed (Fig. 6. 7-B). This kinetics is rather similar to that from amorphous silica to coesite at 450 ℃ (Fig. 6. 1-B).

The morphological changes of the crystals formed were found to be also similar to those which were observed at 450 ℃ on amorphous silica. Some micrographs are shown in Fig. 6. 8. After 48 h, the spherulitic aggregates of quartz crystals with the size of 20 $\sim$ 200 μm were found to be scattered in amorphous matrix (Fig. 6. 8). In these aggregates, the c-axes of quartz crystals oriented mostly to

the radial direction. The crystals of coesite were also developed radially from the center of the quartz spherulites (Fig. 6. 8-A). It seemed likely that before the transition to coesite the radial arrangement of quartz crystals were destroyed to be random. After 96 h, lath-shaped and needle-like crystals of coesite were developed, but the spherulitic texture remained even after the complete transition to coesite.

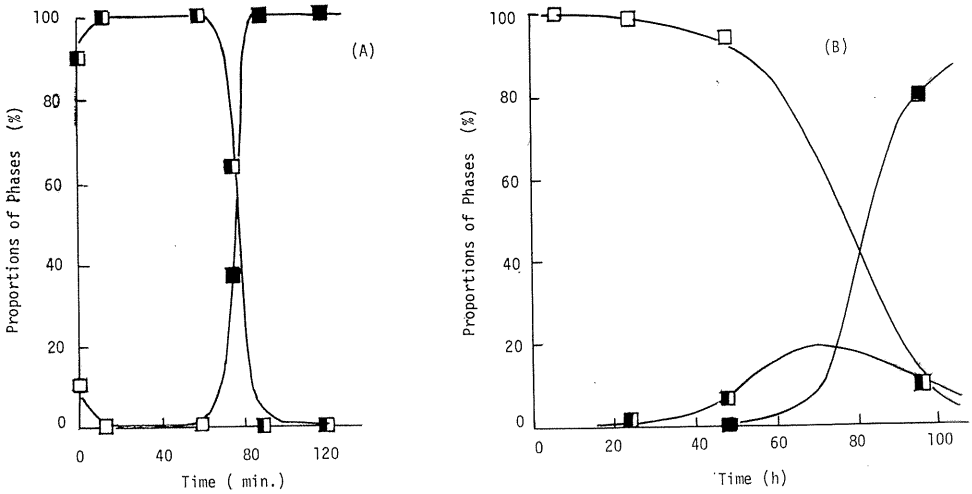

Fig. 6. 7. Variations with time in proportion of silica glass (open marks), quartz (half-filled) and coesite (filled) under 30 kbars.
A: with 10 wt% water at 450℃,
B: without water at 600℃.

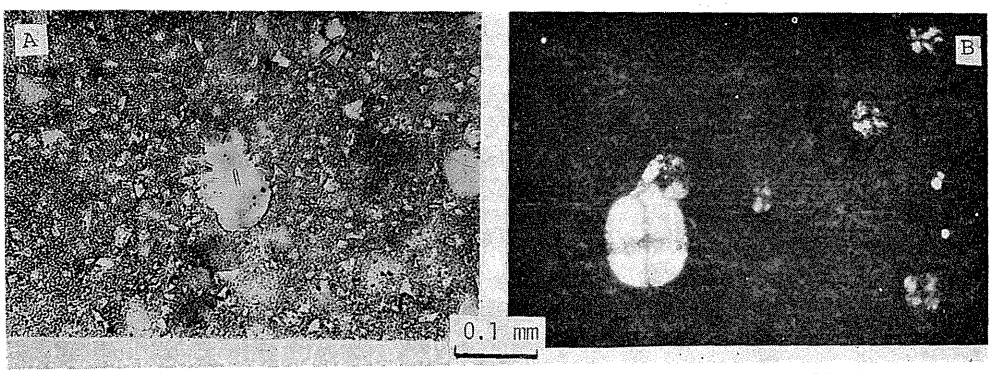

Fig. 6. 8. Micrographs of crystals formed from silica glass under 30 kbars at 600℃ without water.
A: for 48 h (under open nicol),
B: for 48 h (under crossed nicols).

In the existence of 10 wt% water at 450℃, however, the kinetics (Fig. 6. 7-A) and morphological changes to coesite from silica glass was found to be similar to the case from amorphous silica under the same condition, i. e. at 450℃ with 10 wt% water (Fig. 6. 1-A).

6. 3. 4. Crystallization of Coesite from Quartz and Crystal Morphology

The formation of coesite from quartz under 30 kbars without water was retarded in comparison with other starting materials, amorphous silica and silica glass. Some representative results are shown in Table 6. 1. At 450℃ even after 96 h, the starting material of quartz remained unaltered in a powdered state. However, the broadening of X-ray diffraction profiles and the undulatory extinction under polarizing microscope were observed on quartz crystals after heating, suggesting the increase in strain and the pulverization of quartz crystals. The single phase of coesite was obtained from quartz only after 2 h at 700℃. The crystals of coesite formed were in granular shape with the size of 2 ~ 5 μm (Fig. 6. 9-A).

Table 6. 1. Some representative results of heating of quartz under 30 kbars pressure and crystal morphology.

temperature (℃)	heating time (h)	phases (%)		crystal morphology
		quartz	coesite	
450	96	100	0	quartz crystals with homogeneous size of 0.2 μm, undulatory extinction
600	96	100	0	
650	24	100	0	
700	24	0	100	coesite with the size of 2 ~ 5 μm
800	24	0	100	coesite with the size of 5 ~ 10 μm

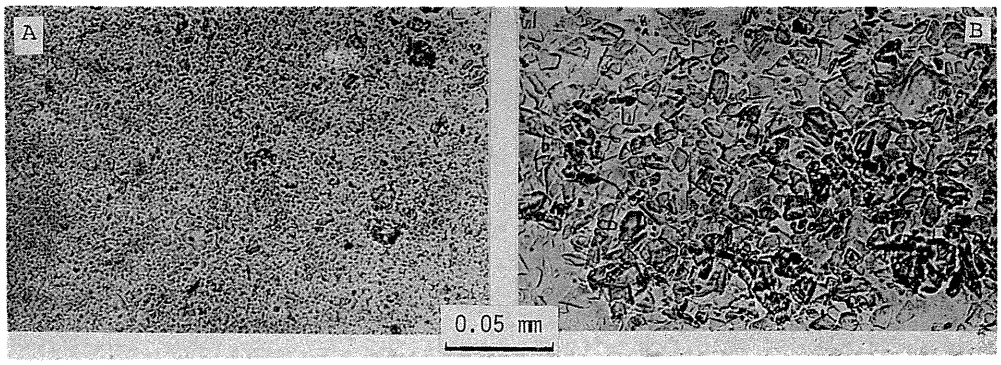

Fig. 6. 9. Micrographs of coesite formed from quartz.
A: at 700℃ for 24 h without water (under open nicol)
B: at 450℃ for 4 h with 10 wt% water (under open nicol)

In the existence of 10 wt% water at 450℃ under 30 kbars pressure, coesite crystallized after an induction period of about 3 h. The variation in proportion of coesite is shown in Fig. 6. 10. After 4 h, 90% of the starting material of quartz was converted into the granular crystals of coesite with the size of 20 ~ 40 μm (Fig. 6. 9-B). Under scanning electron microscope, the sintering of quartz crystal without water was observed. The surface of the quartz crystals was more rough under anhydrous condition than under hydrous one.

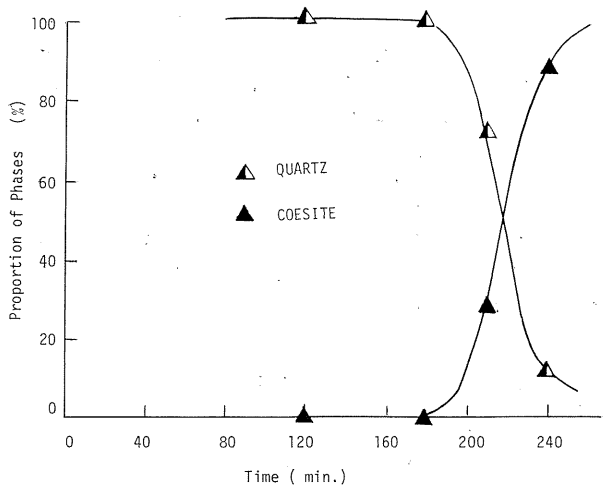

Fig. 6. 10. Variation with time in proportion of coesite formed from quartz under 30 kbars at 450 ℃ with 10 wt% water.

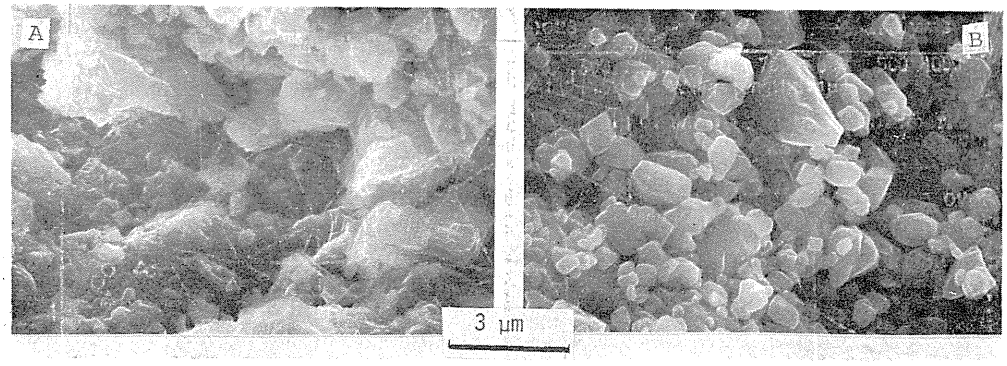

Fig. 6. 11. SEM micrographs of quartz.
A : without water under 30 kbars at 450℃ for 48 h,
B : with 10 wt% water under 30 kbars at 450℃ for 2 h.

6. 4. Discussion

6. 4. 1. Effect of Water on Crystallization of Coesite

Under anhydrous condition, the formation rate of coesite under 30 kbars pressure is different from the starting materials; amorphous silica is converted completely to coesite even at 450℃ after 96 h, but silica glass and quartz need higher temperatures as 600° and 700 °C, respectively, for complete transition to coesite. During the crystallization of coesite from amorphous silica and silica glass, the formation of spherulitic aggregates of intermediate phase of quartz is observed. The spherulitic aggregates formed in the silica glass appear to have better orientation of quartz crystals in the radial direction and are less in number than those in amorphous silica, probably due to the slow rate of transition of silica glass to metastable quartz. The formation of spherulitic aggregates may be explained by

the surface tension developed in amorphous state, similar to the devitrification of glass (Hillert & Hillert, 1970). Mostly from the center of the spherulites, the growth of coesite crystals is found to start. Therefore, the formation of spherulites and also the orientation in spherulites of quartz crystals control the morphology and size of crystals of stable coesite.

Under hydrous condition, i. e. in the presence of 4 ~ 16 wt% water, on the other hand, no difference in the formation rate of coesite is observed between amorphous silica and silica glass. They transform to coesite much faster than quartz. The process of transition of metastable quartz to stable coesite seems to be the rate-determining step. Since kinetic curves for the formation of coesite is unable to be referred to a parabolic law, no long range diffusion process should be involved in the crystallization of coesite. In the present work, therefore, the formation rate of coesite is analyzed by adopting the linear law (Verduch, 1958), which has been commonly used for the rate-determining process of interfacial reaction. The nucleation period, the nucleation rate and the growth rate of stable coesite from metastable quartz evaluated from the slope of the formation curves are summarized in Table 6. 2.

Table 6. 2. Formation of coesite from various starting materials at 450 ℃ under 30 kbars with 10 wt % water.

Starting materials	Crystallite size of metastable quartz (Å)	Nucleation period (min)	Nucleation rate (s^{-1})	Growth rate (s^{-1})
Amorphous silica Silica glass	200 ~ 500	60	2.8×10^{-4}	7.5×10^{-2}
Quartz	5000	80	9.3×10^{-5}	2.8×10^{-2}

The crystallite size of metastable quartz is also shown in the same table. Both the nucleation rate and the growth rate of coesite crystals are found to be larger for amorphous silica and silica glass than for quartz. This difference in the rates may be due to the smaller particle size of metastable quartz formed from amorphous silica and glass than that from quartz. It has been well known that the dimension and the microstructure of the starting crystal affect both speed and temperature of its phase transition (Buerger, 1953).

The crystals of coesite formed from the amorphous phases, amorphous silica and silica glass, through metastable quartz under anhydrous condition have an elongated shape with heterogeneous size and appears to be defective, but well sintered. The crystals formed under hydrous condition, however, are granular in shape, homogeneous in size and also less defective. In the presence of more than 10 wt% of water, the granular crystals of metastable quartz and also of stable coesite are obtained from all starting materials. Water prevents the aggregation of metastable quartz crystals. Even in the presence of water, the elongated crystals and penetration twins of coesite are often observed at the beginning of crystallization, but they disappear after the prolonged heating. These experimental results suggest the dissolution and precipitation through a solvent of water as the growth mechanism of coesite. This mechanism may be understood from the fact that water of even

4 wt% is largely enough to cover the surface of quartz and coesite grains by water layer of few tens molecular thickness.

Using quartz as a starting material, the penetration twins and needle-like crystals of coesite are hardly observed even under anhydrous condition. Random orientation and rigid boundaries of the original quartz particles may prevent the aggregation of grains of metastable quartz and the preferential growth of coesite.

On the kinetics obtained under 40 kbars pressure at 450, 500 and 600 ℃ without water and at 200, 250 and 300 ℃ with 10 wt% water, the approximate values of rate constants k_A and k_C were tried to evaluate by assuming the first order rate process for each step, i. e. from amorphous silica to intermediate quartz and from quartz to stable coesite. The values obtained are plotted as a function of the inverse of temperature, 1/T, in Fig. 6. 12. In spite of only three points of experiments, the differences in the slope of the temperature dependence of each constants k_A and k_C between under anhydrous and hydrous conditions are evident. The activation energies estimated are summarized in Table 6. 3. Under anhydrous condition, both rate constants are roughly equal as expected qualitatively from the kinetic curves. This result of semi-quantitative analysis is also coincide with the qualitative discussion on the crystallization kinetics which have been obtained on another starting material "amorphous silica A" as shown in Chapter 4 and summarized in Fig. 4. 7. The result that the activation energy for the step from amorphous silica to quartz is a little larger than that for the other step from quartz to coesite is also consistent with the previous result that at 900 ℃, $k_A \gg k_C$ though $k_A \approx k_C$ at 550℃ (Fig. 4. 7). Under hydrous condition, activation energies for both steps become much smaller than under anhydrous condition. The larger value of k_A than k_C (k_A is larger than k_C by roughly 6～40) agrees with the previous result that the first step is remarkably accelerated in the presence of water.

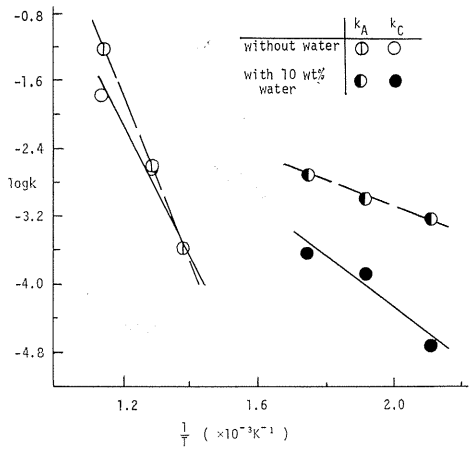

Fig. 6. 12. Arrhenius plots of rate constants k_A and k_C under 40 kbars without water and with 10 wt% water.

Table 6. 3. Activation energies (kcal/mole) for the crystallization of coesite from amorphous silica under 40 kbars

step	temperature range examined (℃)	activation energy (kcal/mole)	
		without water	with 10 wt% water
amorphous silica $\xrightarrow{k_A}$ quartz	450 ～ 600	47	5
quartz $\xrightarrow{k_C}$ coesite	200 ～ 300	37	17

6. 4. 2. Crystallization of Coesite in the Relation to the Solid-Liquid Boundary of Water

In order to understand the effect of water for crystallization of coesite under high temperatures and high pressures, we tried to discuss the observed formation rate in the relation to the solid-liquid boundary of water. As shown in Fig. 6. 3, the proportion of coesite formed under various pressures for 1 h heating changes rather abruptly with temperature. In Fig. 6. 13, the approximate proportion of

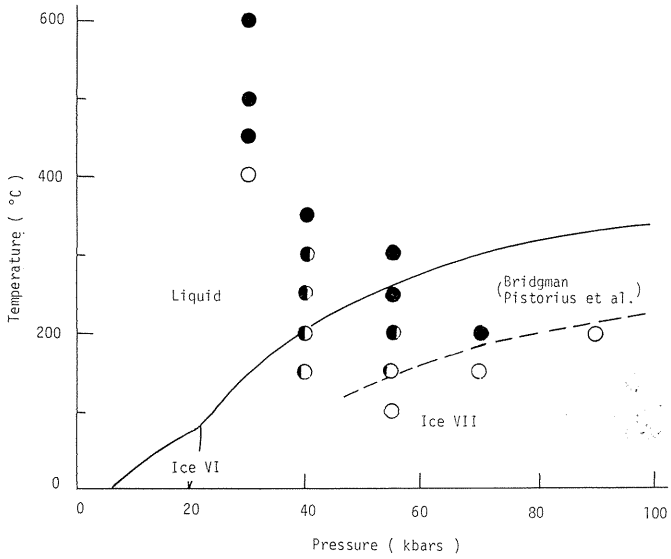

Fig. 6. 13. Relation between the crystallization of coesite in the presence of 10 wt% water and equilibrium solid-liquid boundary of water.

coesite formed in the presence of 10 wt% water after 1 h is shown on the pressure-temperature diagram. The equilibrium boundaries between some phases of water were overlapped in the figure.

At the temperature of 200℃, the amount of coesite increases with increasing pressure up to 70 kbars, being 100% under 70 kbars. Under higher pressure of 90 kbars, however, even trace of coesite is unable to be detected. At 150℃, the amount of coesite tends to decrease with increasing pressure, and under 70 kbars pressure no coesite was detected. Under 55 kbars, no coesite was formed at 100℃. Therefore, we may assume rather sharp boundary for the formation of coesite under the pressure around 80 kbars at 200℃ around 60 kbars at 150℃ and at less than 55 kbars at 100℃, as shown by the broken line in Fig. 6. 13. We note that this assumed boundary is close and roughly parallel to the equilibrium solid-liquid boundary of water (Bridgman, 1937; Pistorius et al., 1963). It is well-known that silica is dissolved into water under high temperature and high pressure. So, it looks reasonable that the solid-liquid boundary shifts to lower temperature due to the dissolution of silica. Combining with the idea that coesite crystals grow by the mechanism of dissolution and precipitation through a solvent of water, the assumed

boundary (broken line in Fig. 6. 13) is likely to be a solid-liquid boundary of water in the presence of silica. Even though we knew only approximate position of the solid-liquid boundary of water, it is interesting that the remarkable acceleration effect of water is found only in the region of temperature and pressure where water is in liquid or fluid state.

Chapter 7. Twinning in Coesite

7. 1. Introduction

In the crystals of coesite synthesized, simple contact twins with (021) plane as the composition and twin planes are observed (Ramsdell, 1955; Sclar et al., 1962). Ramsdell (1955) also observed (100) twinning. Khitarov et al. (1957) reported the cross-like intergrown crystals of coesite, but they did not give any morphological evidence.

Here, two new types of penetration twin in coesite crystals synthesized, were described, in addition to the simple contact twins with euhedral faces, and the formation conditions for these new penetration twins were also discussed.

7. 2. Experimental

The cell arrangement used for the girdle-type high-pressure apparatus was shown in Fig. 2. 1. The pressure-temperature conditions applied were in the ranges of the pressure of 23 ~ 31 kbars and of the temperature of 400 ~ 1300 ℃. The starting materials were two kinds of amorphous silica, one prepared by hydrolysis of $SiCl_4$ ("amorphous silica A") and the other by hydrolysis of silicon ethoxide ("amorphous silica B"), natural quartzite ("quartz A") and cristobalite which was prepared by hydrolysis of silicon ethoxide ("cristobalite").

7. 3. Results and Discussion

In Fig. 7. 1 and 7. 2, two new types of penetration twin of coesite are shown together with respective stereographic projections. The twin plane is $(\bar{1}21)$ for the former and $(\bar{2}33)$ for the latter, which are determined from the axial ratio of coesite, i. e. a : b : c=0. 58 : 1 : 0. 58. Under crossed nicols, both types consist of two idiomorphic individuals of approximately equal size, each individual being elongated parallel to the c-axis. The optical orientation of coesite is $X=b$ and $Z\wedge c=4\sim6°$. The optical angle $2V_Z$ was determined with a universal stage to be 66. 5°. Some of the crystals had (010) cleavage plane (Fig. 7. 2). Subconcoidal fractures were also observed perpendicular to the c-axis, as shown by Sclar et al. (1962).

These penetration twins occurred more frequently in coesite prepared under anhydrous rather than hydrous conditions, and when the abrupt crystallization of coesite occurred after long induction period. On the coesite samples prepared under anhydrous condition from amorphous silica subjected to 23 kbars pressure and 900 ℃ for 10 h, the micrographs are shown in Fig. 7. 3, which suggest the morphological development of coesite crystals. Under this condition (23 kbars, 900 ℃, anhydrous), the induction period of 5 h was needed for crystallization of coesite (see Chapter 4 and Fig. 4. 2). After the induction period, coesite crystallized abruptly in the matrix of metastable quartz and grew mostly along the c-axis. In the grown crystals, subconcoidal fractures occurred perpendicular to the growth direction (see

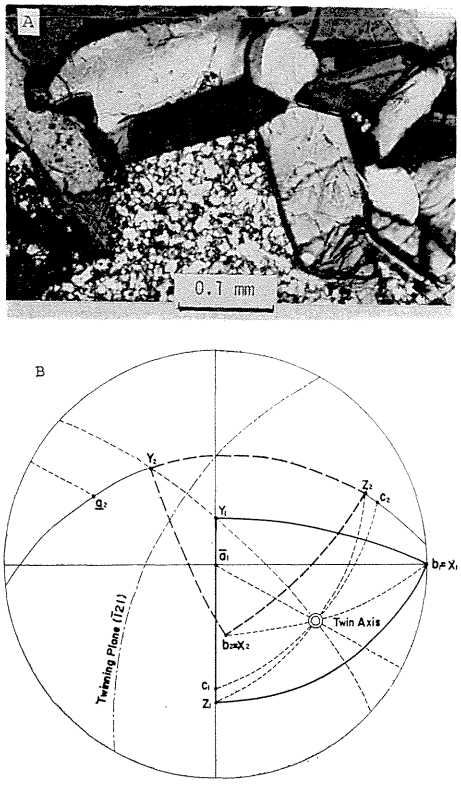

Fig. 7. 1. Penetration twin of coesite with ($\bar{1}21$) twin plane (A) and its stereographic projection (B). The crystals prepared from cristobalite under 30 kbars at 900 ℃ in the presence of 10 wt% water after 1 h.

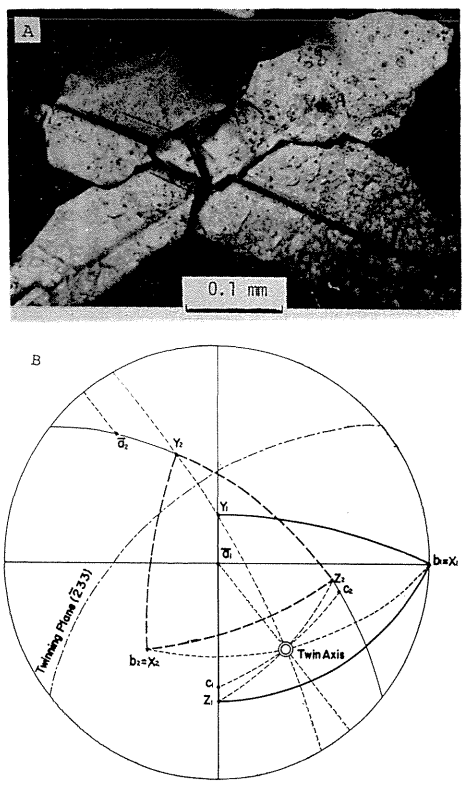

Fig. 7. 2. Penetration twin with ($\bar{2}33$) twin plane and its stereographic projection. (010) cleavage is also observed. The crystals prepared from cristobalite under 30 kbars at 900 ℃ in the presence of 10 wt% water after 12 h.

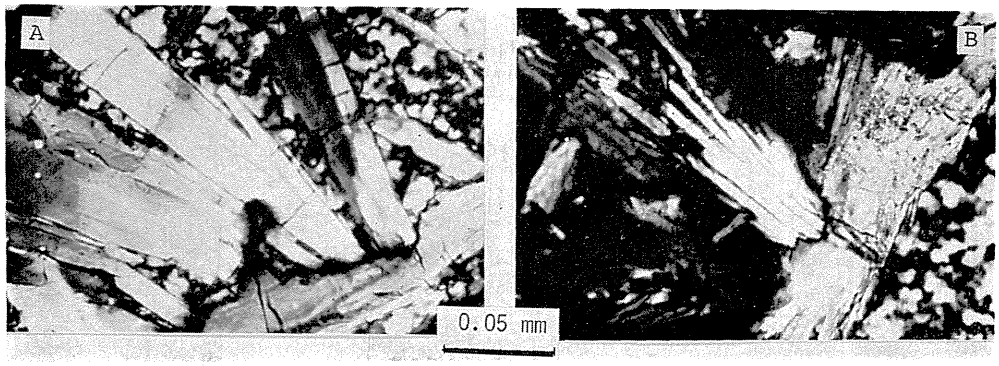

Fig. 7. 3. Micrographs suggesting the formation mechanism of penetration twins. The crystals prepared from amorphous silica under 23 kbars at 900 ℃ after 10 h.

Chapter 5). These subconcoidal fractures could be the growth center of coesite and a number of crystals started to grow along the c-axis, as shown in Fig. 7. 3-B. The two crystals which satisfied the special relation of mutual orientation seemed to be penetration twins, as shown in Figs. 7. 1 and 7. 2.

In coesite prepared anhydrously from amorphous silica under 30 kbars pressure at 600℃ for 3 h, a great number of penetration twins developed. In the presence of 4 wt% water under the same condition, the euhedral crystals with rather homogeneous sizes were observed in addition to the penetration twins of about 0.03 mm long (Fig. 7. 4-A). In the presence of more amount of water (16 wt%), the penetration twins were difficult to be found and most crystals of coesite were discrete polyhedra with the homogeneous size of about 0.02 mm (Fig. 7. 4-B). In the coesite crystals prepared from cristobalite under 30 kbars pressure at 900℃ with 10 wt% water after 185 h, the simple contact twins with tabular kite shape (Fig. 7. 5-A) were observed together with the penetration twins (Fig. 7. 5-B) and polyhedral

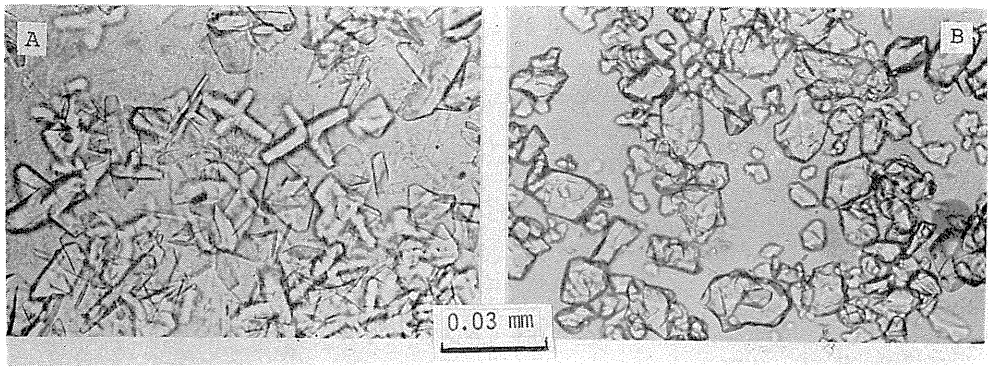

Fig. 7. 4. The crystals of coesite prepared from amorphous silica under 30 kbars at 600℃ in the presence of 4 wt% water after 10 min (A) and in the presence of 16 wt% water after 60 min (B).

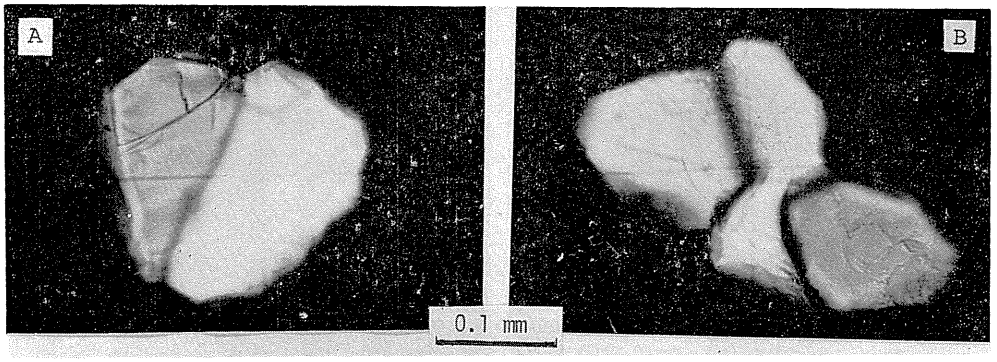

Fig. 7. 5. The contact twins with kite shape (A) and the penetration twin (B) for med from cristobalite under 30 kbars at 900 ℃ after 185 h in the presence of 10 wt% water.

single crystals. Arndt & Rombach (1976) reported only penetration twins during

the crystallization of coesite from aqueous solution. In the present work, we obtained not only penetration but also contact twins.

The growth of twins along the c-axis occurred preferentially perpendicular to the direction of compression (Fig. 7. 6). The growth of the crystal was retarded parallel to the direction of compression (Fig. 7. 6-B). Such oriented growth of twins of coesite seems partially due to the shearing stress, which is inherent in the girdle-type high-pressure apparatus used (see Chapter 2 and 3; Naka et al., 1972a).

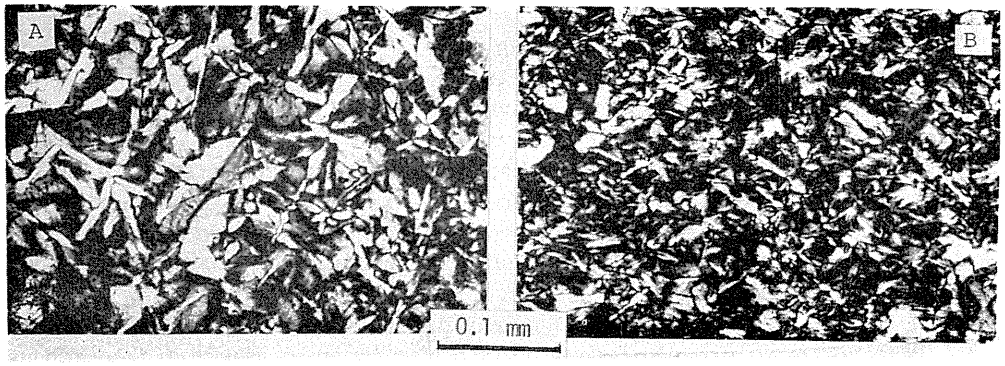

Fig. 7. 6. Preferential growth of coesite crystals with the c-axis perpendicular to compressing direction. (A) in the plane perpendicular to compressing direction and (B) in the plane parallel to compressing direction. The crystals prepared from amorphous silica under 30 kbars at 600 ℃ without water after 3 h.

The growth of the twins was also affeted by treatment temperature. No twins were observed in the coesite crystals synthesized from quartz under 31 kbars at 900℃ without water before 1 h. However, twins were observed in the samples prepared under the same conditions after 2 h and also at 1300 ℃ after 1 h. At high temperatures and after long times of heating, abrupt occurrence of subconcoidal fractures (see Chapter 5) and abundant nucleation of coesite at grain boundaries of quartz were likely to result in the formation of the penetration twins.

The penetration twins observed seem to be formed by the preferential growth of coesite crystals along the c-axis, reducing the shear. Under hydrous condition, the probability of formation of twins decreases probably due to the restraint of preferential growth of crystals along the particular crystallographic direction by the reduction of shear in the pressure cell. The formation of penetration twins is also controlled by the starting materials and it may be related to the formation and stability of the aggregates of metastable quartz, as discussed in Chapter 6.

Chapter 8. Crystal Growth of Coesite

8. 1. Introduction

In the preceding chapters, the crystallization of coesite from various starting materials was elucidated by kinetic and morphological studies. The crystallization

process from amorphous state of silica to coesite was described as a consecutive process through intermediate phase of metastable quartz and was accelerated remarkably in the presence of water. The mechanism of accelerating effect of water seemed to be a dissolution and precipitation of amorphous silica to intermediate quartz and also of quartz to stable coesite. The crystal morphology of intermediate quartz had close relation to that of stable coesite.

In the present chapter, the preliminary results on crystal growth of coesite under high temperature and high pressure were presented.

8. 2. Experimental

The starting materials used were amorphous silica and quartz: the former was prepared by hydrolysis of silicon ethoxide and described as "amorphous silica B" in Chapter 2, the latter was synthetic quartz, "quartz B". The cell arrangement of the girdle-type high-pressure apparatus was shown in Fig. 2. 2.

The crystal growth of coesite was carried out at the temperature of 900 ℃ under 30 kbars pressure. Under this pressure-temperature condition, coesite was known to be stable phase and the transition from each starting materials to coesite was found to finish within 3 h under anhydrous condition (see Chapter 4). Under hydrous condition, the transition to coesite was reasonably supposed to be much faster. The heating rate of 900 ℃/min and compressing rate of about 1 kb/min were kept constant. Distilled water or 0. 5 N solution of NaOH of 6 μl (about 10 wt% of the sample) was added. After heating, the samples were quenched under compression. The sizes, average width and thickness, of the coesite crystals formed were measured under an optical microscope.

8. 3. Results and Discussion

As has been shown in Chapter 6, the crystals of coesite formed under anhydrous condition are sintered and have greyish colour. From observations on thin sections, many penetration and polysynthetic twins were found (see Chapter 5). By heating with water, however, the samples consisted of small discrete crystals of coesite. The crystals formed under hydrous condition were rather transparent and less defective. Many bulky crystals with euhedral faces were observed in the samples, as shown in Fig. 8. 1. Pseudohexagonal platy and lath-shaped crystals, similar to those reported by Sclar et al. (1962) were also found.

The sizes, width and thickness, of the coesite crystals are plotted in Fig. 8. 2 as a function of heating time at 900 ℃ under 30 kbars in the presence of 10 wt% water. The sizes of crystals and their changes with time are found to be different from the starting materials, although all of the starting materials transform to coesite already in short time of heating. From amorphous silica, both width and thickness of the crystals increase gradually with the increase in heating time and the number of the euhedral crystals also increases. From quartz, the apparent width is a little bigger than from amorphous silica, and shows shallow maximum. Before the maximum, the crystals formed are as defective as those formed under anhydrous condition. After passing the maximum in width, the probability of finding the euhedral crystals increases and it increses with increasing heating time.

In the presence of 10 wt% of the 0. 5 N solution of NaOH, somewhat large crystals of coesite were obtained, as shown in Fig. 8. 3. From the observation of thin sections, the crystals formed from amorphous silica were found to contain larger amounts of cleavage and penetration twin, and to be rich in number of crys-

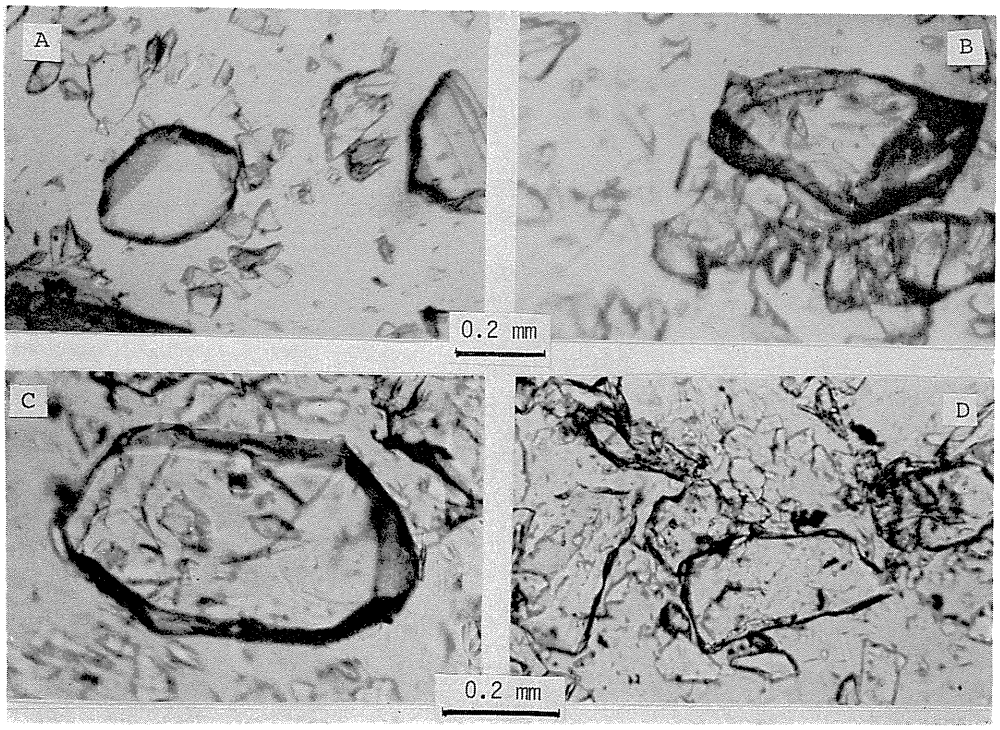

Fig. 8. 1. Micrographs of the coesite crystals formed from amorphous silica (A and B) and quartz (C and D) at 900℃ under 30 kbars pressure with 10 wt% water after 48 h.

tals with higher degree of elongation than those from quartz. The variations of sizes of crystals with heating time are shown in Fig. 8. 4. Starting from amorphous silica, a much more rapid increase of crystal size with heating time is observed in the presence of NaOH solution than of pure water.

From the experimental results described above, the water has a role of flux for crystal growth of coesite under high temperatures and high pressures. Only preliminary results have been obtained, but the possibility to grow large single crystals of coesite by using the flux of water or alkalin solution is verified. Recently, Arndt and Rombach (1976) reported the growth of large crystals of coesite under similar pressure-temperature conditions, of which morphological characteristics are exactly the same as described in the present paper. From the present results related to crystal growth of coesite, we clarify another role of water, i. e. a flux for crystal growth, under high temperatures and high pressures.

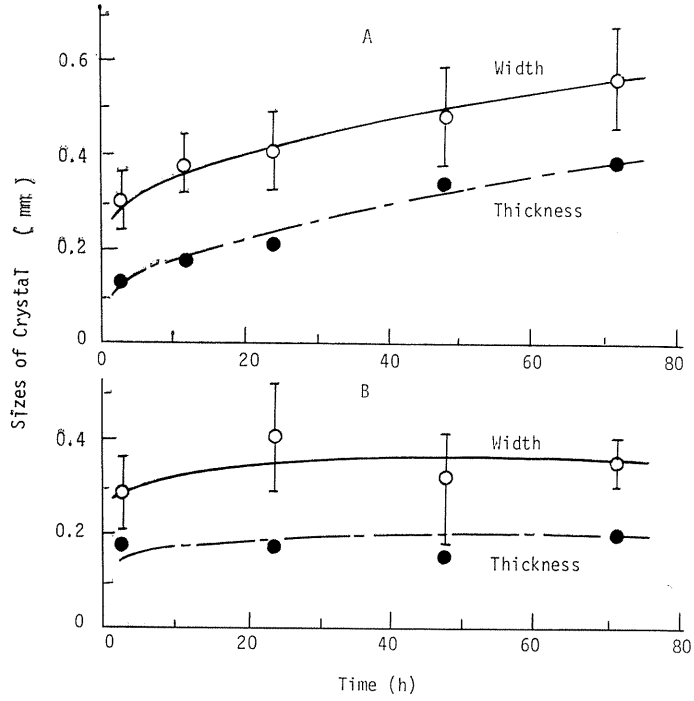

Fig. 8. 2. Variations of size of coesite crystals with heating time under 30 kbars at 900 ℃ in the presence of 10 wt% water from amorphous silica (A) and from quartz (B).

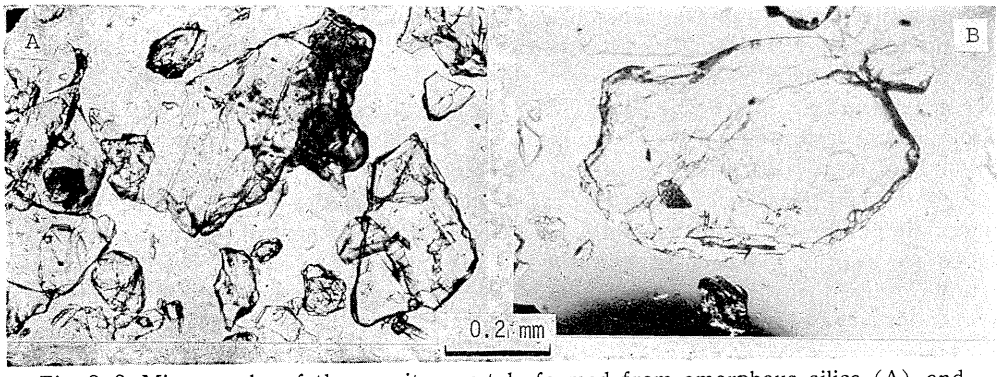

Fig. 8. 3. Micrographs of the coesite crystals formed from amorphous silica (A) and quartz (B) at 900 ℃ under 30 kbars pressure for 24 h with 10 wt% of 0.5 N NaOH.

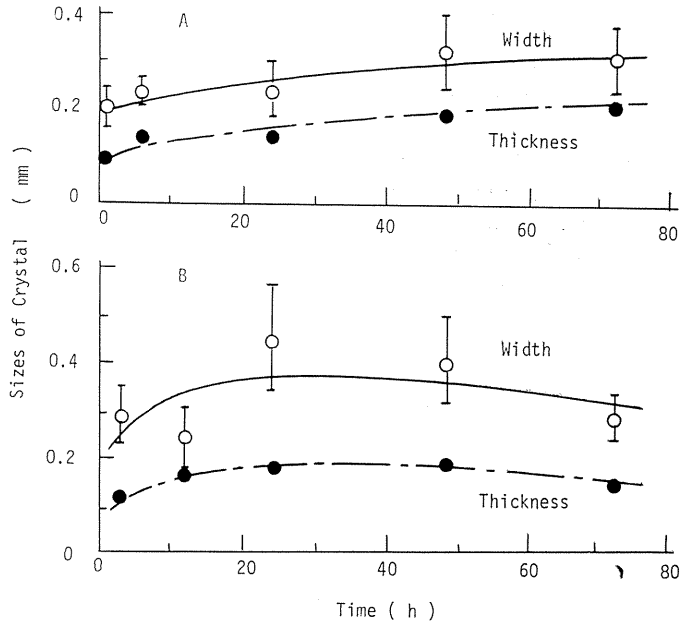

Fig. 8. 4. Variations of size of coesite crystals with heating time under 30 kbars at 900 ℃ in the presence of 10 wt% of 0.5 N NaOH from amorphous silica (A) and from quartz (B).

Chapter 9. Conclusive Remarks

The purposes of the present work are the systematic studies of crystallization of coesite, which is one of high-pressure modifications of silica, in the girdle-type high-pressure apparatus and presentation of fundamental information on high-temperature and high-pressure solution growth of coesite. The results obtained in the present work are summarized as follows:

1. We are able to obtain the pressure up to 90 kbars and the temperature up to 1600 ℃ in a relatively large volume for sample in the girdle-type high-pressure apparatus by using a proper cell arrangement. In spite of the lack of strict hydrostaticity of pressure, this apparatus is powerfull for the studies of crystallizaton process and the growth of single crystals because the different conditions of hydrostaticity can be realized by adding some liquid or by the selection of appropriate pressure-transmitting medium. The facility for attaining high pressures and the long life of the apparatus are also advantage of this apparatus.
2. The distribution of pressure in the cell has been changed by the addition of water and by using different pressure-transmitting media around the sample in order to understand the effect of shear on the transition between quartz and coesite. Shear has very important role for the phase transitions. Summarizing the published results obtained by different apparatus, shear is found to shift the equilibrium line toward lower pressure.
3. The process of crystallization of coesite has been studied kinetically at 550 ~

900 ℃ under 23 ~ 55 kbars pressure using amorphous silica and quartz as starting materials. On the transition from amorphous silica to coesite, strained quartz is observed as an intermediate phase. The rate process is consecutive through quartz. On the formation of coesite from starting quartz, a similar strained quartz is recognized as an intermediate stage from the broadness of the diffraction lines of the quartz phase. The crystallization rate of coesite from amorphous silica increases with increasing pressure up to 40 kbars at 550 ℃, but then decreases under pressures as high as 55 kbars. At 900℃, the crystallization of coesite from intermediate quartz is faster than that from amorphous silica under 23 and 31 kbars but slower under 40 kbars. These results are explained by assuming the dependencies of the rate constants for each step on temperature and pressure.

4. Morphological development of coesite crystals obtained at 550 ~ 1300 ℃ under 20 ~ 55 kbars is found to be strongly influenced by the state of aggregates of intermediate quartz. At the beginning of crystallization, fine particles of metastable quartz with 7~8 μm in size occurs from amorphous silica under 31 kbars pressure at 900℃ of which temperature-pressure condition is pretty close to the phase boundary between quartz and coesite, and, in the matrix of these quartz particles, a small amount of pseudohexagonal platelets and many needle-like lath-shaped crystals of coesite are found. The pseudohexagonal platelets grow along the c-axis and consequently rather bulky crystals with lath-shape are mostly found after long time heating. The size of coesite crystals decreases with increasing pressure and with decreasing temperature. From quartz, the needle-like crystals with smaller size are mostly obtained. The difference in morphological development of coesite crystals formed from amorphous silica and quartz is probably due to the shear exerted on the sample.
5. The effect of water on crystallization process of coesite has been studied at 100 ~ 700 ℃ under 30 ~ 90 kbars by using different starting materials (amorphous silica, silica glass and quartz) from the kinetic and morphological points of view. The presence of water is found to have remarkable effects not only on the kinetics of crystallization of coesite but also on the morphology of metastable quartz and consequently of coesite crystals. Under anhydrous conditions, from amorphous silica and silica glass, the spherulitic aggregates of metastable quartz appear. The crystals of coesite are developed mostly at the center of the spherulites of quartz as the elongated shape with different sizes and look defective. From synthetic quartz, however, only small amount of spherulitic aggregates of quartz is found after long time heating and granular crystals of coesite are obtained. Under hydrous conditions, granular crystals of coesite with homogeneous size are developed rapidly at 450 ℃ from both amorphous silica and silica glass through the discrete particles of metastable quartz.

   The accelerating effect of water on crystallization of coesite is remarkable under certain pressure-temperature conditions (below 80 kbars at 200 ℃ and below 60 kbars at 150 ℃, for examples) where water is in liquid or fluid state.
6. Two new types of penetration twins are found in coesite prepared from amorphous silica, cristobalite and quartz under 30 kbars pressure at 400 ~ 1300 ℃, in addition to the simple contact twin reported previously. The twin planes of two penetrpation twins are $(\bar{1}21)$ and $(\bar{2}33)$, respectively. The effects of added water and temperature on twin growth are studied. Occurrence of these twins may be attributed to preferential growth along the c-axis of coesite.

7. The preliminary experiments on the crystal growth of coesite under hydrous conditions have been carried out under 30 kbars pressure at 900 ℃ by using amorphous silica and quartz as starting materials. In the presence of 10 wt% water, the crystals formed seem to be less defective and some of them have euhedral faces. The crystals of coesite have relatively large distribution in size, but large crystals are bulky and euhedral. The sizes of the crystal increase gradually with the increase in heating time. By the addition of about 10 wt% of a 0.5 N NaOH solution, the effect of water is accelerated.
8. From the experimental results on crystallization of coesite in the presence of water, three roles of water are recognized; 1) the reduction of the shear exerted on the sample under high-pressure, 2) the acceleration of transitions from amorphous silica to intermediate phase of metastable quartz and from metastable quartz to stable coesite, and 3) the flux for crystal growth of coesite.

Acknowledgement

The authors wish to thank Prof. Kanenori SUWA, Faculty of Science, Nagoya University, who worked with us on the part of microscopic observation of twins. They also thank to all of the members of Synthetic Crystal Research Laboratory for their encouragement and assistance for the present work. Financial supports from the Ministry of Education (1971, 1972 and 1976) are acknowledged.

References

Akimoto, S. & Syono, Y., J. Geophys. Res., **74**, 1653 (1969).
Araki, T. & Zoltai, T., Z. Krist., **129**, 381 (1969).
Arndt, J. & Rombach, N., J. Cryst. Growth, **35**, 28 (1976).
Böhler, R. & Arndt, J., Contrib. Mineral. Petrol., **48**, 149 (1974).
Bohn, E. & Stöber, W., Neues Jahrb. Mineral. Monatsch., **1966**, 89 (1966).
Boyd, F. R., Bell, P. M., England, J. L. & Gilbert, M. C., Carnegie Inst. Washington, Yearb., **65**, 410 (1967).
Boyd, F. R. & England, J. L., J. Geophys. Res., **65**, 749 (1960).
Bridgman, P. W., J. Chem. Phys., **5**, 964 (1937).
Buerger, M. J., "Phase Transformation in Solids", pp. 183-211, Edited by Smoluchowski, R., Mayer, J. E. & Weyl, W. A., Wiley, New York, (1953).
Bundy, F. P., "Modern Very High Pressure Techniques", pp. 1-24, Edited by Wentorf, Jr. R. H., Butterworths, London, (1962).
Chaklader, A. C. D. & Roberts, A. L. J. Am. Ceram. Soc, **44**, 35 (1961).
Chao, E. C. T., Shoemaker, E. M. & Madsen, B. M., Science, **132**, 220 (1960).
Chao, E. C. T., Fahey, J. J., Litter, J. & Milton, D. J., J. Geophys. Res., **67**, 419 (1962).
Coes, Jr., L., Science, **118**, 131 (1953).
Cohen, L. H. & Klement, W. Jr., J. Geophys. Res., **72**, 4245 (1969).
Cohen, L. H., Klement, Jr., W. & Kennedy, G. C., Phys. Rev., **145**, 519 (1966).
Dachille, F. & Roy, R., Z. Krist., **111**, 451 (1959).
Dachille, F., Zeto, R. J. & Roy, R., Science, **140**, 991 (1963).
Daniels, W. B. & Jones, M. T., Rev. Sci. Instrum., **32**, 885 (1961).
De Carli, P. S. & Jamieson, J. C., J. Chem. Phys., **31**, 1675 (1959).
Gigl, P. D. & Dachille, F., Meteoritics, **4**, 123 (1968).

Green, Ⅱ., H. W., J. Geophys. Res., **77**, 2478 (1972).
Green, T. H., Ringwood, A. E. & Major, A., J. Geophys. Res., **71**, 3589 (1966).
Griggs, D. T. & Kennedy, G. C., Amer. J. Sci., **254**, 722 (1956).
Hillert, L. & Hillert, M., J. Mat. Sci., **5**, 610 (1970).
Holm, J. L., Kleppa, O. J. & Westrum, E. F., Geochim. Cosmochim. Acta, **31**, 2289 (1967).
Kameyama, T. & Naka, S., Bull. Chem. Soc. Japan, **49**, 92 (1976).
Khitarov, N. I., Slutsky, A. B. & Arsenieva, R. V., Geokhimija, **8**, 666 (1957).
Kitahara, S. & Kennedy, G. C., J. Geophys. Res., **69**, 5395 (1964).
Kracek, F. C., "Phase Transformation in Solids", pp. 257-277, Edited by Smoluchowaski, R., Mayer, J. E. & Weyl, W. A., Wiley, New York, (1953).
Livshits, L. D., Larintov, L. V., Delitsin, I. S., Petrov, V. P. & Svintitskich, V. E., High Temp.-High Press., **4**, 311 (1972).
MacDonald, G. J. F., Amer. J. Sci., **254**, 713 (1956).
Mackenzie, J. D., J. Amer. Ceram. Soc., **46**, 461 (1963).
Mayer, H. O. A., Carnegie Inst. Washington Yearb., **66**, 446 (1968).
Naka, S., Hanawa, T. & Noda, T., Nippon Kagaku Kaishi, **1**, 722 (1972a).
Naka, S., Ito, S. & Inagaki, M., J. Amer. Ceram. Soc. **55**, 323 (1972b).
Naka, S., Inagaki, M., Kameyama, T. & Suwa, K., J. Cryst. Growth, **24/25**, 614 (1974a).
Naka, S., Ito, S. & Inagaki, M., J. Am. Ceram. Soc., **57**, 217 (1974b).
Naka, S., Kameyama, T., Ito, S. & Inagaki, M., Chem. Letters, **1974**, 1313 (1974c).
Naka, S. & Kameyama, T., J. Am. Ceram. Soc., **57**, 499 (1974).
Naka, S., Lameyama, T. & Suwa, K., Am. Mineralog., **60**, 726 (1975).
Nichols. S., J. Sci. Instrum., Series 2, **2**, 506 (1969).
Pistorius, C. W. F. T., Pistorius, M. C., Blakey, J. P. & Admiral, L. T., J. Chem. Physics, **38**, 600 (1963).
Ramsdell, L. S., Am. Mineral., **40**, 975 (1955).
Roy, R. & Frushour, R. H., J. Am. Ceram. Soc., **54**, 589 (1971).
Sclar, C. B., Carrison, L. C. & Schwartz, C. M., Am. Mineral., **47**, 1292 (1962).
Skinner, B. J. & Fahey, J. J., J. Geophys. Res., **68**, 5595 (1963).
Sosman, R. B., "Phases of Silica", Rutger Univ. Press., New Brunswick, N. Y., (1965).
Stishov, S. M. & Popova, S. W., Geokhimija, **10**, 837 (1961).
Stöffler, D., J. Geophys. Res., **76**, 5474 (1971).
Takahashi, T., "High-Pressure Measurement", pp. 240-249, Edited by Giardini, A. A. & Lloyd, F. C., Butterworth, Washington, D. C., (1963).
Ubbelohde, A. R., Quart. Rev., **41**, 246 (1957).
Uhlman, D. R., Hays, J. F. & Turnbull, D., Phys. Chem. Glasses, **7**, 159 (1966).
Verduch, A. G., J. Am. Ceram. Soc., **41**, 427 (1958).
Wagstaff, F. E., Brown, S. D. & Cutler, I. B., Phys. Chem. Glasses, **5**, 76 (1964).
Wagstaff, F. E. & Richards, K. J., J. Am. Ceram. Soc., **49**, 118 (1966).
Young, A. P., Robins, P. B. & Schwartz, C. M., "High-Pressure Measurement", pp. 262-273, Edited by Giardini. A. A. & Lloyd, F. C., Butterworth, Washington, D. C., (1963).
Zeto, Z. J., Dachille, F. & Roy, R., Am. Ceram. Soc. Bull., **41**, 245 (1962),
abstract. Zolta, T. & Buerger, M. J., Z. Krist. **111**, 129 (1959).